

FULL PAPER

Exploration of the nitrogen heterocyclic periphery around the core of the advanced FFA1 agonist fasiglifam (TAK-875)

Alexey Lukin¹ | Anna Bakholdina¹ | Nikolay Zhurilo¹ |
Oleksandra Onopchenko² | Elena Zhuravel² | Sergey Zozulya^{2,3}  |
Maxim Gureev⁴  | Alexander Safrygin⁵  | Mikhail Krasavin⁵ 

¹Lomonosov Institute of Fine Chemical Technologies, MIREA–Russian Technological University, Moscow, Russian Federation

²Enamine Ltd., Kyiv, Ukraine

³Taras Shevchenko National University, Kyiv, Ukraine

⁴I. M. Sechenov First Moscow State Medical University, Moscow, Russian Federation

⁵Institute of Chemistry, Saint Petersburg State University, Saint Petersburg, Russian Federation

Correspondence

Mikhail Krasavin, Institute of Chemistry, Saint Petersburg State University, Saint Petersburg, Russian Federation, 199034.
Email: m.krasavin@spbu.ru

Funding information

Russian Foundation for Basic Research, Grant/Award Number: 19-33-90169

Abstract

Three types of heterocyclic moieties—piperidines fused to a heteroaromatic moiety—were explored as potential periphery motifs for the pharmacophoric core of fasiglifam (TAK-875), with fasiglifam being the most advanced agonist of free fatty acid receptor 1, a promising target for therapeutic intervention in type 2 diabetes. Several observed structure–activity relationship trends were corroborated by *in silico* docking results. Balanced selection based on potency and Caco-2 permeability advanced six compounds to cellular efficacy tests (glucose-stimulated insulin secretion in rat insulinoma INS1E cells). This led to the nomination of compound **16a** (LK1408, 3-[4-({4-[(3-[(2-fluorobenzyl)oxy]methyl)-1-methyl-1,4,6,7-tetrahydro-5H-pyrazolo[4,3-c]pyridin-5-yl)methyl]benzyl}oxy)phenyl]propanoic acid hydrochloride) as the lead for further development.

KEYWORDS

FFA1 receptor, free fatty acids, glucose-stimulated insulin secretion, GPR40, heterocyclic periphery, hyperglycemia, type 2 diabetes mellitus

1 | INTRODUCTION

The G-protein-coupled receptor GPR40 was de-orphaned in 2003 and renamed as free fatty acid receptor 1 (FFA1), owing to its activation by medium- to long-chain free fatty acids as endogenous ligands.^[1] The physiological significance of this activation was established shortly thereafter by demonstrating that binding of a free fatty acid to FFA1 is crucial for regulating secretion of insulin in pancreatic β -cells and, thus, to maintain glucose homeostasis. The uniqueness of this regulatory mechanism was also revealed, which lies in the generally low expression levels of FFA1 in the normoglycemic state. However, once the glucose levels rise (as in diabetic hyperglycemia), there is also an increase in the expression of FFA1. Moreover, as soon as insulin excretion normalizes the glucose levels, the expression levels of FFA1 also revert to the normal low. This makes FFA1 an ideal target for therapeutic intervention in pathological hyperglycemic states such as type 2 diabetes mellitus (T2DM),

as activation of FFA1 by exogenous agonists carries little risk of leading to hypoglycemia, even if the drug remains in circulation after normalization of the glucose levels.^[2]

These observations about FFA1 prompted numerous industry and academic research teams to focus on the validation of this receptor as a principally new antidiabetic target as well as on the discovery of a number of agonists that were reported in the literature during the decade that followed after FFA1 de-orphaning.^[3] However, this area of drug research was adversely impacted in December 2013 by the discontinuation of phase III clinical trials of Takeda's fasiglifam (TAK-875), the most advanced drug candidate at the time, due to reports of idiosyncratic liver toxicity observed within an extended population of patients. Although there is no evidence that this adverse effect was target-related, the fasiglifam setback (and substantial financial losses are inevitable if a drug fails in such an advanced development phase) led to a sharp decrease in the research efforts worldwide aimed at bringing new FFA1 agonists

to the market as a treatment for T2DM.^[4] The cumulative discovery results in this area have been summarized in several recent comprehensive reviews.^[5] However, at the time of preparing this manuscript, only one phase I clinical trial was underway—compound P11187 of the undisclosed structure by Piramal.^[5a] The apparent inactivity in this area is disappointing, as the proof of principle of activating FFA1 to achieve a positive clinical outcome in T2DM patients was, in fact, achieved in the course of clinical investigation of fasiglifam.^[6] The hepatotoxicity of the latter is almost unanimously linked to the highly lipophilic^[7] character of the molecule rather than its action at the receptor, which is primarily expressed in the pancreas and in the brain.^[8] Thus, the principal focus of medicinal chemistry research toward new FFA1 agonists, which continues predominantly in academic laboratories, is on the development of less lipophilic compounds that possibly do not exhibit adverse effects on the liver.^[9]

The pursuit of less lipophilic FFA1 agonists may seem like a sort of “tug of war,” as a ligand’s lipophilicity is known to drive its affinity to the target whose endogenous ligand (free fatty acid) is itself quite lipophilic.^[10] Hence, the FFA1 agonist structure should be modified toward decreasing $\log P$ with care, so as not to lose the on-target activity altogether. Typically, this is achieved via either employing more polar appendages around the 3-phenylpropionic acid pharmacophore (as in compounds **1**^[11] and **2**^[12] where fasiglifam’s benzyloxy group is replaced with a thiazole and an oxazole congener, respectively) or by replacing the said core altogether with higher polarity isosteres: such a “scaffold-hopping” exercise is exemplified by compounds **3**^[13] and **4**^[14] (Figure 1).

Our efforts toward the development of less lipophilic FFA1 agonists have recently focused on the former approach, that is, varying the polar periphery without changing fasiglifam’s basic 3-(4-benzyloxy)phenylpropionic acid scaffold.^[15–17] In some cases, however, total elimination of centroids of lipophilicity from the peripheral motifs led to a complete ablation of potency (as was the case with compound **5**). This loss of affinity to the receptor could be drastically reversed by bringing back lipophilic aromatic (as in compounds **6**) or even adding polar heteroaromatic groups (as in compound **7**). This restoration of potency was shown to be only partly due to new hydrophobic interactions with L54_{2,51}, L135_{4,54}, and V81_{3,27} of the receptor; more considerable (particularly in the case of **7**) was the additional π stacking interaction with W131_{4,50} (Figure 2).^[15–17]

In this study, we aimed to continue exploiting the strategy of fine-tuning the periphery around the basic 3-(4-benzyloxy)phenylpropionic acid scaffold of fasiglifam (TAK-875) to arrive at novel agonists that could be considered as the next generation of FFA1 agonists devoid of overly high lipophilicity and thus carrying less potential risk of hepatotoxicity in vivo, which was the likely cause for fasiglifam’s failure in the clinical development. Mindful of the importance of counterbalancing the addition of polar heterocyclic motifs with aromatic appendages capable of building a network of hydrophobic (free fatty acid-like) and π stacking interactions with the protein target, we designed three types of appendages. Capitalizing upon the successful use of piperidine peripheral motifs,^[15–17] we set off to explore piperidine-fused pyrazole **8**, 2-pyridone **9**, and 2-alkoxypyridine **10**, which could be elaborated into potential FFA1 agonists via reductive amination reaction with aldehyde

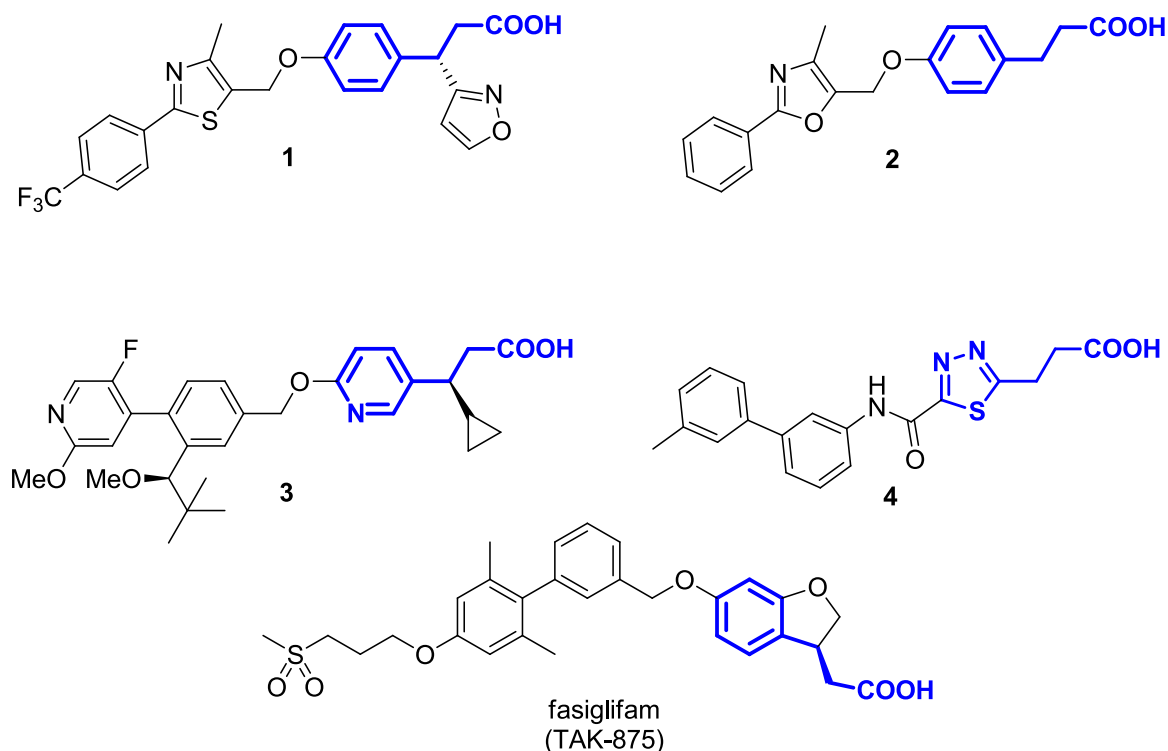
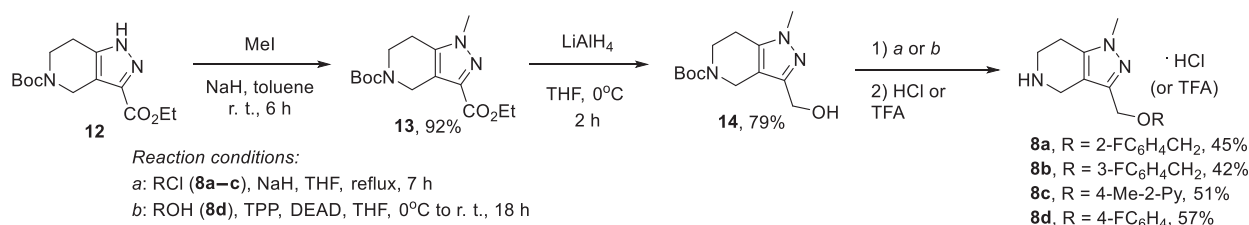


FIGURE 1 Polar appendage (**1**, **2**) and scaffold-hopping (**3**, **4**) approaches toward less lipophilic FFA1 agonists



SCHEME 1 Preparation of the pyrazole-fused piperidines **8a–d**

2-methoxyethyl bromide, both of which gave a sole *N*-alkylation product in a low yield), there was the formation of both *N*- and *O*-alkylation products that were separated chromatographically, whereupon the Boc group was removed by treatment with 4 M HCl solution in 1,4-dioxane to give compounds **9** and **10** as hydrochloride salts (Scheme 2). The regiochemistry of alkylation was confirmed by comparing the correlation spectra (COSY) of both regioisomers (see electrospray ionization [ESI] for such comparison made for the **9g/10g** pair).

All fused piperidines, **9a–g**, **10a–b**, and **10e–g**, thus obtained were employed in the preparation of final, fully elaborated FFA1 agonist **16**, as shown in Scheme 3. The yields of the final products are provided in Table 1 (Section 2.2). Unfortunately, attempts to prepare compound **16** from piperidines **9e–g** and **10b** of purity that would be adequate for biological testing failed.

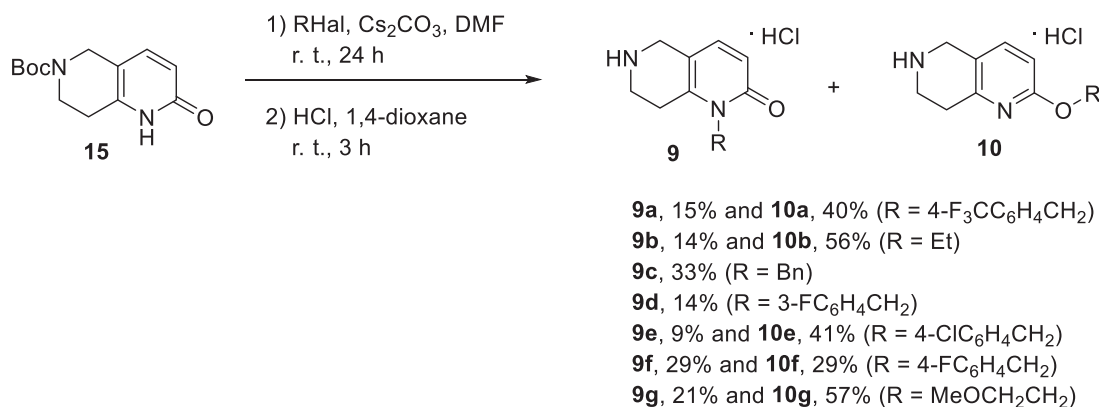
2.2 | Biological activity

Potential FFA1 agonists **16a–l**, synthesized as described above, were tested for their ability to activate FFA1 using the calcium flux assay employing Chinese hamster ovary (CHO) cells engineered to stably express human FFA1. All compounds were tested in a concentration–response mode to calculate the respective EC₅₀ values and determine the percentage of maximum efficacy achieved for active compounds, relative to the commercially available reference FFA1 agonist GW9508.^[21] Additionally, compounds' cell membrane permeability was assessed in human epithelial colorectal adenocarcinoma (Caco-2) cells^[22] in comparison with the reference compounds

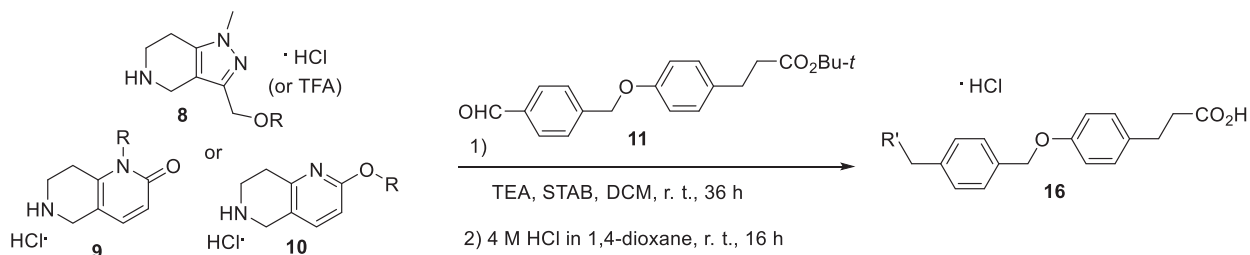
propranolol, quinidine, and atenolol^[23] that displayed high (P_{app}^{AB} , $14.9 \pm 1.4 \text{ cm} \cdot \text{s}^{-1} \cdot 10^{-6}$), medium (P_{app}^{AB} , $11.6 \pm 0.8 \text{ cm} \cdot \text{s}^{-1} \cdot 10^{-6}$), and low (P_{app}^{AB} , $0.2 \pm 0.04 \text{ cm} \cdot \text{s}^{-1} \cdot 10^{-6}$) permeability in this assay, respectively (Table 1).

To our delight, all compounds prepared and investigated in this study demonstrated potent agonism with respect to FFA1 receptor, with nine compounds residing in the sub-micromolar range. At the same time, some generalizations with respect to structure–activity relationships (SAR) could be drawn. In the *N*-alkylated 5,6,7,8-tetrahydro-1,6-naphthyridin-2(1H)-one series (obtainable from building blocks **9**), bulky benzyl groups (as in **16e,g,h**) reduced the affinity to the receptor (only a small ethyl group in **16f** was tolerated). Although they were somewhat similar in topology to each other, pyrazole compounds (**16a–d**) demonstrated generally lower potency as compared with 2-alkoxy-pyridines (**16i–l**). The reasons for both SAR trends have been investigated with the aid of in silico modeling (vide infra).

On the basis of the combination of potency and predicted cell membrane permeability, six compounds (**16a–c**, **16f**, and **16i,j**) were selected for further profiling. Specifically, we aimed to establish if these compounds are capable of stimulating insulin secretion from rat insulinoma INS1E cells^[24] in the presence of a fixed concentration of glucose. To be able to compare the effects of our compounds with those produced by the reference FFA1 agonist GW9805,^[21] we determined the glucose concentration at which the addition of 10 μM of GW9805 would lead to a significant increase in insulin levels. As shown in Figure 4a, at 0.5 mM glucose concentration, the addition of GW9805 had no effect; however, the increase in the



SCHEME 2 Preparation of the 2-pyridone- and 2-alkoxy-pyridine-fused piperidines **9** and **10**



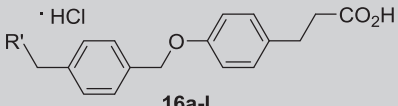
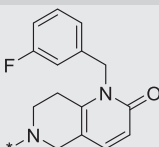
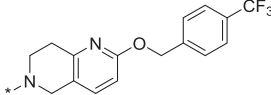
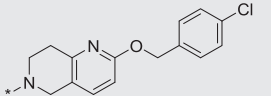
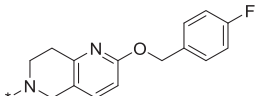
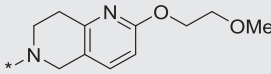
SCHEME 3 Preparation of final FFA1 agonist **16**. DCM, dichloromethane; STAB, sodium triacetoxyborohydride; TEA, triethylamine, TFA, trifluoroacetic acid

TABLE 1 FFA1 agonists **16a–l** studied in this study

Compound	R'	8–10	Yield (%)	FFA1; EC ₅₀ ± SD (μM) ^a	% Efficacy ^b	Caco-2; P _{app} ^{AB} (cm·s ⁻¹ ·10 ⁻⁶) ^c	cLog P ^d
16a–l							
16a (LK1408)		8a	56	0.65 ± 0.12	95.0	10.4 ± 2.2	5.40
16b		8b	25	0.60 ± 0.08	89.2	9.2 ± 0.1	5.42
16c		8d	74	0.61 ± 0.10	93.4	7.0 ± 0.3	5.45
16d		8c	87	0.43 ± 0.03	90.2	ND	4.78
16e		9a	33	1.74 ± 0.18	88.4	3.4 ± 0.2	5.27
16f		9b	42	0.69 ± 0.07	93.5	4.6 ± 0.3	3.16
16g		9c	20	2.97 ± 0.43	70.5	5.7 ± 1.2	4.38

(Continues)

TABLE 1 (Continued)

Compound	R ¹	8-10	Yield (%)	FFA1; EC ₅₀ ± SD (μM) ^a	% Efficacy ^b	Caco-2; P _{app} ^{AB} (cm·s ⁻¹ ·10 ⁻⁶) ^c	cLog P ^d
 16a-l							
16h		9d	32	1.13 ± 0.11	100.3	5.8 ± 0.3	4.51
16i		10a	56	0.32 ± 0.09	90.3	<0.1	5.22
16j		10e	16	0.33 ± 0.04	64.5	11.4 ± 0.3	5.01
16k		10f	27	0.37 ± 0.09	94.9	0.9 ± 0.5	4.49
16l		10g	14	0.15 ± 0.05	68.5	<0.1	3.34

Abbreviation: ND, not determined.

^aEach value is an average of $n = 4$.

^bRelative to GW9508^[21] (5 μM).

^cEach value is an average of $n = 2$, measured at $c = 10$ μM.

^dCalculated using www.molinspiration.com.

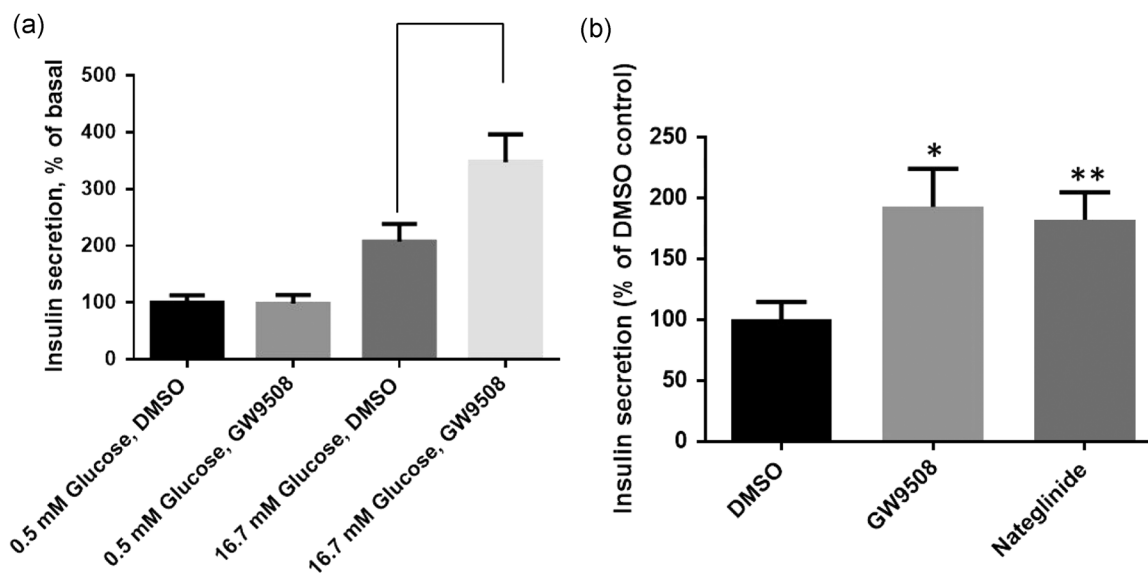


FIGURE 4 Insulin secretion in INS1E cells (a) in the presence of 10 μM GW9805 at 0.5 mM and 16.7 mM concentration of glucose and (b) in the presence of 10 μM GW9805 and 20 μM nateglinide at 16.7 mM concentration of glucose. Data shown are the mean ± SD of values from three replicate samples. * $p < .05$; ** $p < .01$, compared with dimethyl sulfoxide (DMSO) control

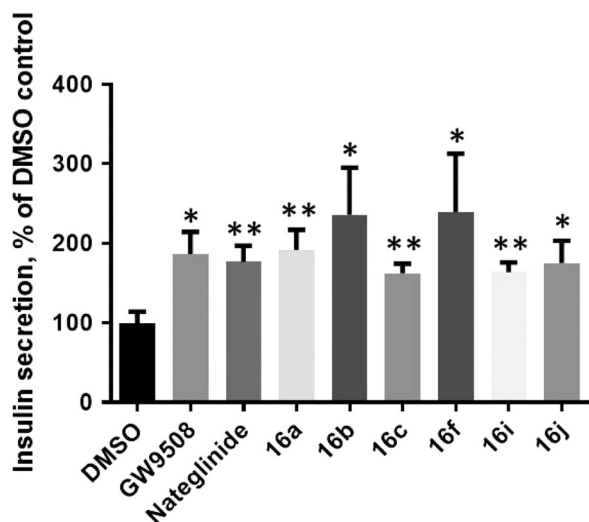


FIGURE 5 Insulin secretion in INS1E cells treated with six frontrunner compounds (10 μ M), GW9805 (10 μ M), and nateglinide (20 μ M) in the presence of 16.7 mM glucose. Data shown are the mean \pm SD of values from three replicate samples. The experiment was repeated twice with similar results (data not shown). * $p < .05$; ** $p < .01$, compared with dimethyl sulfoxide (DMSO) control

concentration to 16.7 mM produced a significant elevation of the agonist-induced insulin levels. Hence, our agonists were subsequently tested in comparison to GW9805 (10 μ M) as well as to nateglinide (20 mM), a clinically used glucose-lowering agent operating via the blockage of ATP-dependent potassium channels in the membrane of pancreatic β cells.^[25] The latter drug also produced a significant elevation of insulin levels in INS1E cells in the presence of 16.7 mM glucose (Figure 4b).

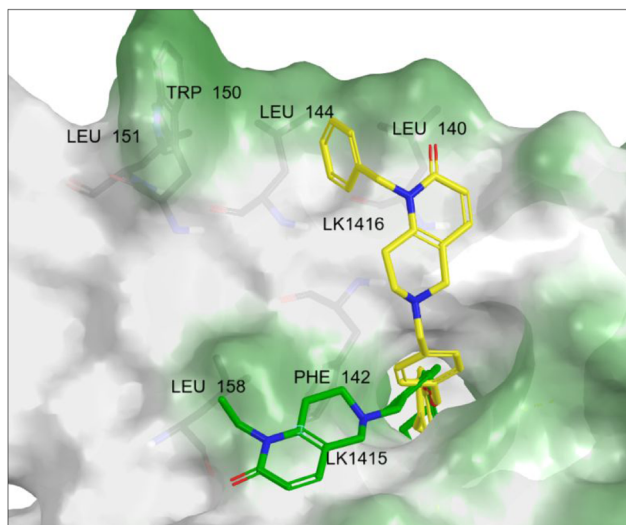


FIGURE 6 Binding poses of compounds **16f** (green) and **16g** (yellow) within the hydrophobic region of FFA1 endogenous ligand binding (partial view of the tail binding)

All six frontrunner compounds (**16a–c**, **16f**, and **16i,j**) were tested in INS1E cells in the presence of 16.7 mM glucose (Figure 5). To our delight, all six compounds appeared to reproduce the effects of both GW9805 and nateglinide on insulin secretion. Moreover, compound **16a** (LK1408), whose profile most closely resembled that of the two reference drugs with a high statistical significance ($p < .01$), was tested in the same assay in a dose-dependent manner and its EC_{50} was determined to be in the range of 0.3–0.7 nM in three independent experiments.

2.3 | In silico modeling

We employed in silico docking to rationalize some of the most pronounced SAR trends observed within the set of FFA1 agonists **16a–l**. In particular, we were curious to understand the structural reasons for (i) the more than fourfold decrease in potency on going from *N*-ethyl to *N*-benzyl substitution pattern in compounds **16f** and **16g**, (ii) the even more pronounced increase in potency on relocating the 4-(trifluoromethyl)benzyl group from the nitrogen atom in **16e** to the oxygen atom in **16i**, and (iii) the similar difference in potency between *N*-alkyl derivative **16f** and its closest *O*-alkyl congener **16l**.

2.3.1 | Comparative docking of **16f** and **16g**

The introduction of the lipophilic phenyl substituent (**16g**) in lieu of the methyl group in **16f** appears to change the profile of hydrophobic contacts by the molecular periphery of FFA1 agonists. For instance, the benzyl substituent of **16g** is involved in the network of interactions with the hydrophobic surface delineated by Leu140, Leu144, Leu151, and Trp150. The total incremental contribution of this hydrophobic interaction to the binding energy was calculated as 320.87 kcal/mol. In contrast, the hydrophobic interactions by the ethyl substituent of **16f** contributed only 40.04 kcal/mol (Figure 6).

These observations are consistent with the generally more favorable component analysis performed for both ligands using the MM-GBSA method (Table 2) where the most significant differences in Coulomb energy and energy of strained interactions are evident.

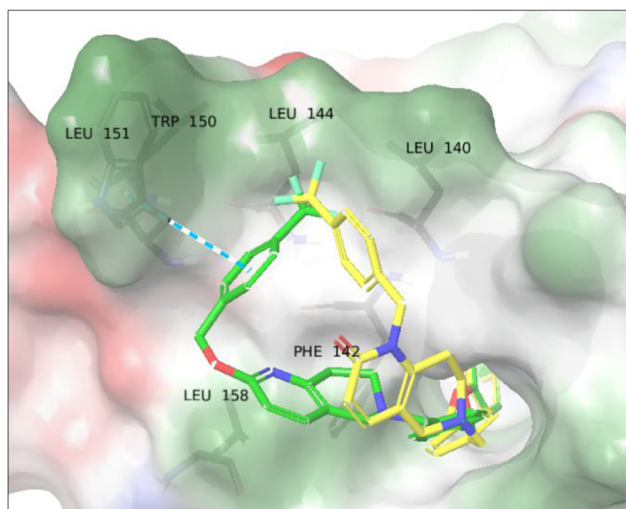
2.3.2 | Comparative docking of **16e** and **16i**

A comparison of the activity profile of groups of agonists **16a–d** and **16i–l**, both of which have a “linear,” extended tail topology, with that of *N*-alkyl derivatives **16e–h** having more of an “angular” tail disposition indicates the preferred character of the former ligand shape. However, we were interested in obtaining more accurate docking results, so we corroborated this observation with calculated binding energy values and various components thereof.

Docking of compounds **16e** and **16i**, allowing for a direct comparison of the *N*- and *O*-alkylated series, respectively, revealed that a more effective network of hydrophobic contacts of the

TABLE 2 Binding free energy component calculated for ligands **16f** and **16g** using the MM-GBSA method

Compound	Glide score	ΔG H-bond (kcal/mol)	ΔG Coulomb (kcal/mol)	ΔG Lipo (kcal/mol)	ΔG Strain (kcal/mol)
16f	-9.03	-2.12	-24.54	-38.90	4.71
16g	-9.49	-0.36	-13.28	-39.73	7.95

**FIGURE 7** Binding poses of compounds **16i** (green) and **16e** (yellow); a partial view of the tail binding

O-(4-trifluoro)benzyl tail of **16i** is involved. In contrast to **16e** whose hydrophobic tail only makes hydrophobic contacts with Leu140, Leu144, Leu151, and Trp150, **16i** also forms a π stacking interaction with the latter amino acid residue. Additionally, a greater flexibility of the benzyloxy tails in **16i** allows it to reach into the hydrophobic area, whereas its fused piperidine moiety is an effectively hydrophilic area (Figure 7).

The component analysis of the associated binding energy performed using the MM-GBSA method (Table 3) showed a significantly preferable contribution from the three components—Coulomb, lipophilic, and strained—whereas the hydrogen bonding component remained the same.

2.3.3 | Comparative docking of **16f** and **16i**

Considering that moving bulky benzylic substituents from the nitrogen atom to the oxygen atom of the tetrahydro-1,6-naphthyridin-2-one heterocyclic periphery (**16e** \rightarrow **16i**, vide supra) led to a substantial

TABLE 3 Binding free energy component calculated for ligands **16e** and **16i** using the MM-GBSA method

Compound	Glide score	ΔG H-bond (kcal/mol)	ΔG Coulomb (kcal/mol)	ΔG Lipo (kcal/mol)	ΔG Strain (kcal/mol)
16e	-9.03	-2.12	-24.54	-38.90	4.71
16i	-9.49	-0.36	-13.28	-39.73	7.95

improvement of potency at the FFA1 receptor, we were curious to see what structural reasons could be responsible for a similar potency trend on changing the substitution pattern between **16f** and **16i** (where there was no additional π stacking with Trp150, as was the case with compounds **16i**).

The docking results (Figure 8) indicated that more efficient contacts of the tetrahydro-1,6-naphthyridin-2-one moiety with the hydrophilic area of the receptor is the likely reason for the greater than fourfold higher affinity of **16i** as compared with **16f**.

As was observed previously, the component analysis of the associated binding energy performed using the MM-GBSA method demonstrated a significantly more preferable contribution of the Coulomb and lipophilic components for compound **16i** (Table 4), which is quite in line with the visual inspection of the binding pose.

3 | CONCLUSION

We have widened the range of heterocyclic peripheral motifs that could be employed in combination with the known 3-(4-benzyloxy)phenylpropionic acid scaffold to produce potent ($EC_{50} \sim 10^{-7}$ to 10^{-6} M) and efficacious agonists (as measured in glucose-stimulated insulin excretion assay performed in rat insulinoma INS1E cells). These efforts resulted in the identification of the new lead compound **16a** (LK1408) for further development as potential therapy for type 2 diabetes that is devoid of hypoglycemia risk.

4 | EXPERIMENTAL

4.1 | Chemistry

4.1.1 | General

All reactions were conducted in oven-dried glassware in atmosphere of nitrogen. Melting points were measured with a Buchi B-520 melting point apparatus and were not corrected. Analytical thin-layer

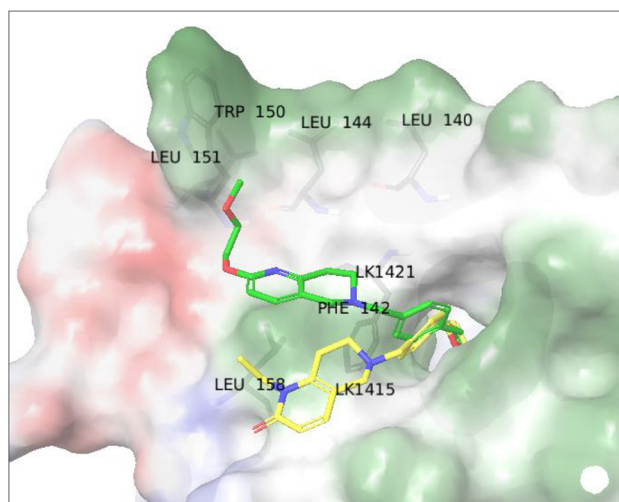


FIGURE 8 Binding poses of compounds **16l** (green) and **16f** (yellow); a partial view of the tail binding

chromatography was carried out on Silufol UV-254 silica gel plates using appropriate mixtures of ethyl acetate and hexane. Compounds were visualized with short-wavelength UV light. The ^1H nuclear magnetic resonance (NMR) and ^{13}C NMR spectra (see Supporting Information) were recorded on Bruker MSL-300 spectrometers in dimethyl sulfoxide ($\text{DMSO}-d_6$) or CDCl_3 using tetramethylsilane as an internal standard. Mass spectra were recorded using Shimadzu LCMS-2020 system with ESI. All reagents and solvents were obtained from commercial sources and used without purification.

All mass spectroscopic measurements required for the determination of ADME properties were performed using the Shimadzu VP HPLC system including vacuum degasser, gradient pumps, reverse phase high-performance liquid chromatography (HPLC) column, column oven, and autosampler. The HPLC system was coupled with a tandem mass spectrometer API 3000 (PE Sciex). The TurbolonSpray ion source was used in both positive and negative ion modes. Acquisition and analysis of the data were performed using Analyst 1.5.2 software (PE Sciex).

The InChI codes of the investigated compounds, together with some biological activity data, are provided as Supporting Information.

4.1.2 | Synthesis of 5-*tert*-butyl 3-ethyl-1-methyl-1,4,6,7-tetrahydro-5H-pyrazolo[4,3-*c*]pyridine-3,5-dicarboxylate (**13**)

To a suspension of sodium hydride (62.5 mmol, 1.5 g) in anhydrous toluene (25 ml), solid 5-*tert*-butyl 3-ethyl-1,4,6,7-tetrahydro-5H-pyrazolo

[4,3-*c*]pyridine-3,5-dicarboxylate (**12**)^[19] (33.9 mmol, 10 g) was added with stirring. Iodomethane (42.4 mmol, 2.64 ml) was then added dropwise and stirring continued for 6 h at room temperature. The progress of the reaction was monitored using thin-layer chromatography and 3% methanol in chloroform as an eluent. The reaction mixture was washed with 5% aq. K_2CO_3 (25 ml), 5% aq. citric acid (25 ml), and water (25 ml). The organic phase was dried over anhydrous sodium sulfate, filtered, and concentrated in vacuo to give the title compound. Yield, 10 g (92%); white solid; m.p. 124.0–124.5°C. ^1H NMR (300 MHz, CDCl_3) δ 4.58 (s, 2H), 4.37 (q, $J = 7.1$ Hz, 2H), 3.80 (s, 3H), 3.70 (t, $J = 5.7$ Hz, 2H), 2.66 (t, $J = 5.6$ Hz, 2H), 1.46 (s, 9H), 1.37 (t, $J = 7.1$ Hz, 3H); ^{13}C NMR (75 MHz, CDCl_3) δ 162.5, 155.1, 138.7, 138.1, 117.8, 80.3, 60.8, 41.5, 40.1, 36.5, 28.5, 22.0, 14.5. High-resolution mass spectrometry (HRMS) (ESI) m/z calcd for $\text{C}_{15}\text{H}_{24}\text{N}_3\text{O}_4$ [$\text{M}+\text{H}^+$] 310.1761 Da, found 310.1767 \pm 0.0015 Da.

4.1.3 | Synthesis of *tert*-butyl 3-(hydroxymethyl)-1-methyl-1,4,6,7-tetrahydro-5H-pyrazolo[4,3-*c*]pyridine-5-carboxylate (**14**)

5-*tert*-Butyl 3-ethyl-1-methyl-1,4,6,7-tetrahydro-5H-pyrazolo[4,3-*c*]pyridine-3,5-dicarboxylate (**13**; 3.1 mmol, 10 g) was dissolved in anhydrous tetrahydrofuran (THF; 50 ml), and LiAlH_4 (26.2 mmol, 1 g) was added in small portions at 0°C. The progress of the reaction was monitored using thin-layer chromatography and 2% methanol in chloroform as an eluent. After the completion of the reaction, water (1 ml), 15% aq. NaOH (1 ml), and again water (3 ml) were successively added, and the resulting

TABLE 4 Binding free-energy component calculated for ligands **16e** and **16i** using the MM-GBSA method

Compound	Glide score	$\Delta\text{G H-bond}$ (kcal/mol)	$\Delta\text{G Coulomb}$ (kcal/mol)	$\Delta\text{G Lipo}$ (kcal/mol)	$\Delta\text{G Strain}$ (kcal/mol)
16f	-9.03	-2.12	-24.54	-38.90	4.71
16l	-9.24	-2.31	-26.30	-39.16	4.34

biphasic mixture was stirred for 2 h at room temperature. The precipitate formed was filtered off and the filtrate was collected and concentrated in vacuo. The residue was dissolved in ethyl acetate (50 ml) and washed with water (20 ml), 5% aq. citric acid (20 ml), and water (20 ml). The organic phase was dried over anhydrous sodium sulfate, filtered, and concentrated in vacuo to give the title compound. Yield, 6.3 g (79%); m.p. 96.0–96.5°C. ^1H NMR (300 MHz, CDCl_3) δ 4.59 (s, 2H), 4.42 (s, 2H), 3.69 (s, 3H), 3.68 (t, $J = 5.6$ Hz, 2H), 2.62 (t, $J = 5.7$ Hz, 2H), 1.46 (s, 9H); ^{13}C NMR (75 MHz, CDCl_3) δ 155.1, 146.5, 138.1, 112.1, 80.2, 57.7, 40.3, 40.3, 35.5, 28.6, 22.0. HRMS (ESI) m/z calcd for $\text{C}_{13}\text{H}_{22}\text{N}_3\text{O}_3$ [$\text{M}+\text{H}^+$] 268.1655 Da, found 268.1651 \pm 0.0020 Da.

4.1.4 | Synthesis of 3-[[2-(2-fluorobenzyl)oxy]-methyl]-1-methyl-4,5,6,7-tetrahydro-1H-pyrazolo[4,3-c]pyridine hydrochloride (8a)

tert-Butyl 3-(hydroxymethyl)-1-methyl-1,4,6,7-tetrahydro-5H-pyrazolo[4,3-c]pyridine-5-carboxylate (**14**; 7.12 mmol, 2 g) was dissolved in anhydrous THF (25 ml), and sodium hydride (8.54 mmol, 0.342 g) was added in small portions. After 15 min stirring at room temperature, 1-(chloromethyl)-2-fluorobenzene (8.54 mmol, 1.23 g) was added and the mixture was heated at reflux for 7 h. The progress of the reaction was monitored using thin-layer chromatography and 50% ethyl acetate in petroleum ether as an eluent. The reaction mixture was washed with 5% aq. K_2CO_3 (25 ml), 5% aq. citric acid (25 ml), and water (25 ml). The organic phase was dried over anhydrous sodium sulfate, filtered, and concentrated in vacuo to give the crude product. The latter was purified by column chromatography. Fractions containing the target material were pooled and concentrated in vacuo, and the residue was dissolved in anhydrous 1,4-dioxane. A 4 M solution of HCl in 1,4-dioxane (2 ml) was added and the mixture was sonicated until a well-formed hydrochloride salt precipitate separated. The latter was filtered off, washed with ether, and air-dried to give the title compound. Yield, 1.5 g (45%); m.p. 145–146°C. ^1H NMR (300 MHz, $\text{DMSO}-d_6$) δ 9.79 (br.s, 2H), 7.49–7.31 (m, 2H), 7.26–7.12 (m, 2H), 4.52 (s, 2H), 4.47 (s, 2H), 4.01 (s, 2H), 3.67 (s, 3H), 3.35–3.28 (m, 2H), 2.92 (t, $J = 5.9$ Hz, 3H); ^{13}C NMR (75 MHz, $\text{DMSO}-d_6$) δ 160.4 (d, $J = 245.3$ Hz), 143.5, 135.7, 130.5 (d, $J = 4.4$ Hz), 130.0 (d, $J = 8.2$ Hz), 125.0 (d, $J = 14.8$ Hz), 124.5 (d, $J = 3.4$ Hz), 115.3 (d, $J = 21.2$ Hz), 107.8, 65.3 (d, $J = 3.4$ Hz), 41.0, 38.9, 35.6, 18.4. HRMS (ESI) m/z calcd for $\text{C}_{15}\text{H}_{19}\text{FN}_3\text{O}$ [$\text{M}+\text{H}^+$] 276.1506 Da, found 276.1503 \pm 0.0010 Da.

4.1.5 | Synthesis of 3-[[3-(3-fluorobenzyl)oxy]-methyl]-1-methyl-4,5,6,7-tetrahydro-1H-pyrazolo[4,3-c]pyridine hydrochloride (8b)

The title compound was synthesized analogously to **8a** using 1-(chloromethyl)-3-fluorobenzene as the alkylating agent. Yield, 1.4 g

(42%); m.p. 139–140°C. ^1H NMR (300 MHz, $\text{DMSO}-d_6$) δ 9.86 (s, 2H), 7.43–7.34 (m, 1H), 7.20–7.02 (m, 3H), 4.48 (s, 2H), 4.46 (s, 2H), 4.03 (t, $J = 4.1$ Hz, 2H), 3.68 (s, 3H), 3.37–3.28 (m, 2H), 2.93 (t, $J = 6.0$ Hz, 2H); ^{13}C NMR (75 MHz, $\text{DMSO}-d_6$) δ 162.2 (d, $J = 243.4$ Hz), 143.5, 141.3 (d, $J = 7.2$ Hz), 135.7, 130.3 (d, $J = 8.3$ Hz), 123.4 (d, $J = 2.6$ Hz), 114.2 (d, $J = 20.9$ Hz), 114.1 (d, $J = 21.5$ Hz), 107.8, 70.50, 6.75, 41.5, 38.8, 35.6, 18.4. HRMS (ESI) m/z calcd for $\text{C}_{15}\text{H}_{19}\text{FN}_3\text{O}$ [$\text{M}+\text{H}^+$] 276.1506 Da, found 276.1504 \pm 0.0020 Da.

4.1.6 | Synthesis of 1-methyl-3-[[4-(4-methylpyridin-2-yl)oxy]methyl]-4,5,6,7-tetrahydro-1H-pyrazolo[4,3-c]pyridine trifluoroacetate (8c)

The title compound was synthesized analogously to **8a** using 2-chloro-4-methylpyridine as an arylating agent. The Boc group was removed using TFA (3 equiv.) in dichloromethane. Yield, 2 g (51%); m.p. 139–140°C. ^1H NMR (300 MHz, $\text{DMSO}-d_6$) δ 9.12 (s, 2H), 8.06 (d, $J = 5.3$ Hz, 1H), 6.88 (d, $J = 5.2$ Hz, 1H), 6.71 (s, 1H), 5.24 (s, 2H), 4.16 (br.s, 2H), 3.71 (s, 3H), 3.47–3.34 (m, 2H), 2.91 (t, $J = 5.9$ Hz, 2H), 2.28 (s, 3H); ^{13}C NMR (75 MHz, $\text{DMSO}-d_6$) δ 162.8, 158.7 (q, $J = 37.3$ Hz), 151.4, 145.7, 142.5, 135.5, 119.0, 115.6 (q, $J = 289.9$ Hz), 110.8, 108.2, 60.4, 40.5, 39.6, 35.7, 20.6, 18.5. HRMS (ESI) m/z calcd for $\text{C}_{14}\text{H}_{19}\text{N}_4\text{O}$ [$\text{M}+\text{H}^+$] 259.1553 Da, found 259.1551 \pm 0.0015 Da.

4.1.7 | Synthesis of 3-[[4-(4-fluorophenoxy)methyl]-1-methyl-4,5,6,7-tetrahydro-1H-pyrazolo[4,3-c]pyridine hydrochloride (8d)

To a solution of *tert*-butyl 3-(hydroxymethyl)-1-methyl-1,4,6,7-tetrahydro-5H-pyrazolo[4,3-c]pyridine-5-carboxylate (**14**; 7.12 mmol, 2 g), 4-fluorophenol (8.54 mmol, 0.95 g), and triphenyl phosphine (7.83 mmol, 2.05 g) in dry THF (50 ml), diisopropylazadecarboxylate (9.40 mmol, 1.64 g) was added at 0°C. The reaction mixture was stirred at room temperature for 18 h and concentrated in vacuo. The residue was purified by column chromatography on silica gel using chloroform as an eluent. Fractions containing the target material were pooled and concentrated in vacuo, and the residue was dissolved in anhydrous 1,4-dioxane. A 4 M solution of HCl in 1,4-dioxane (2 ml) was added and the mixture was sonicated until a well-formed hydrochloride salt precipitate separated. The latter was filtered off, washed with ether, and air-dried to give the title compound. Yield, 2 g (57%); m.p. 139–140°C. ^1H NMR (300 MHz, $\text{DMSO}-d_6$) δ 9.77 (br.s, 2H), 7.15–7.07 (m, 2H), 7.05–6.98 (m, 2H), 4.99 (s, 2H), 4.07 (t, $J = 4.2$ Hz, 2H), 3.70 (s, 3H), 3.37–3.28 (m, 2H), 2.94 (t, $J = 6.0$ Hz, 2H); ^{13}C NMR (75 MHz, $\text{DMSO}-d_6$) δ 156.7 (d, $J = 236.1$ Hz), 154.5, 142.3, 135.7, 116.0, 115.9 (d, $J = 32.3$ Hz), 107.9, 63.4, 40.6, 38.8, 35.6, 18.3. HRMS (ESI) m/z calcd for $\text{C}_{14}\text{H}_{17}\text{FN}_3\text{O}$ [$\text{M}+\text{H}^+$] 262.1305 Da, found 262.1305 \pm 0.0020 Da.

4.1.8 | Synthesis of 1-[4-(trifluoromethyl)benzyl]-5,6,7,8-tetrahydro-1,6-naphthyridin-2(1H)-one hydrochloride (9a) and 2-[[4-(trifluoromethyl)benzyl]oxy]-5,6,7,8-tetrahydro-1,6-naphthyridine hydrochloride (10a)

tert-Butyl 2-oxo-1,5,7,8-tetrahydro-1,6-naphthyridine-6(2H)-carboxylate^[20] (0.8 mmol, 0.2 g; **15**) was dissolved in anhydrous DMF (5 ml). 1-(Chloromethyl)-4-(trifluoromethyl)benzene (0.96 mmol, 0.187 g) was added, followed by cesium carbonate (3.2 mmol, 1.041 g). The reaction mixture was stirred for 24 h. The progress of the reaction was monitored using thin-layer chromatography and 1% methanol in chloroform as an eluent. After the completion of the reaction, the mixture was diluted with water (100 ml) and extracted with ethyl acetate (3 × 20 ml). The organic phase was dried over anhydrous sodium sulfate, filtered, and concentrated in vacuo. The residue was fractionated on silica gel column using 0–3% methanol in chloroform as an eluent. Fractions eluting with R_f 0.5 and R_f 0.2 were pooled and concentrated. Each residue was dissolved in anhydrous 1,4-dioxane. A 4 M solution of HCl in 1,4-dioxane (2 ml) was added and the mixtures were sonicated until well-formed hydrochloride salt precipitates separated. The latter were filtered off, washed with ether, and air-dried to give **9a** and **10a**, respectively.

9a: Yield, 0.048 g (15%); white solid; m.p. 110–111 °C. ¹H NMR (300 MHz, DMSO-*d*₆) δ 9.62 (br.s, 2H), 7.71 (d, *J* = 8.1 Hz, 2H), 7.46–7.30 (m, 3H), 6.51 (d, *J* = 9.4 Hz, 1H), 5.38 (br.s, 2H), 4.00 (s, 2H), 3.27 (br.s, 2H), 2.87 (br.s, 2H); ¹³C NMR (75 MHz, DMSO-*d*₆) δ 161.7, 141.6 (q, *J* = 1.1 Hz), 140.5, 139.2, 127.9 (q, *J* = 31.8 Hz), 127.3, 125.7 (q, *J* = 3.6 Hz), 124.3 (q, *J* = 272.0 Hz), 118.0, 107.6, 45.3, 41.9, 39.4, 30.8. HRMS (ESI) *m/z* calcd for C₁₆H₁₆F₃N₂O [M+H⁺] 309.1209 Da, found 309.1208 ± 0.0020 Da.

10a: Yield, 0.128 g (40%); white solid; m.p. 101–102 °C. ¹H NMR (300 MHz, DMSO-*d*₆) δ 9.85 (br.s, 2H), 7.75–7.65 (m, 4H), 7.62 (d, *J* = 8.5 Hz, 1H), 6.82 (d, *J* = 8.4 Hz, 1H), 5.43 (s, 2H), 4.17 (t, *J* = 3.9 Hz, 2H), 3.45–3.34 (m, 2H), 2.99 (t, *J* = 6.1 Hz, 2H); ¹³C NMR (75 MHz, DMSO-*d*₆) δ 162.0, 149.2, 138.7, 129.7, 128.3 (d, *J* = 31.6 Hz), 126.9, 125.3 (q, *J* = 3.8 Hz), 124.3 (d, *J* = 272.0 Hz), 118.1, 109.4, 45.0, 42.6, 40.6, 23.0. HRMS (ESI) *m/z* calcd for C₁₆H₁₆F₃N₂O [M+H⁺] 309.1209 Da, found 309.1209 ± 0.0020 Da.

4.1.9 | Synthesis of 1-ethyl-5,6,7,8-tetrahydro-1,6-naphthyridin-2(1H)-one hydrochloride (9b) and 2-ethoxy-5,6,7,8-tetrahydro-1,6-naphthyridine hydrochloride (10b)

They were prepared in full analogy to **9a/10a**, except for the use of ethyl bromide as an alkylating agent.

9b: Yield, 0.03 g (14%); white solid; m.p. 93–94 °C. ¹H NMR (300 MHz, DMSO-*d*₆) δ 9.66 (br.s, 2H), 7.27 (d, *J* = 9.4 Hz, 1H), 6.37 (d, *J* = 9.3 Hz, 1H), 4.03–3.91 (m, 4H), 3.42–3.30 (m, 2H), 3.03 (t, *J* = 5.8 Hz, 2H), 1.15 (t, *J* = 7.0 Hz, 3H); ¹³C NMR (75 MHz, DMSO-*d*₆) δ 161.3, 140.2, 138.4, 117.9, 107.0, 79.3, 42.1, 38.1, 22.8, 13.4.

HRMS (ESI) *m/z* calcd for C₁₀H₁₅N₂O [M+H⁺] 179.1178 Da, found 179.1180 ± 0.0015 Da.

10b: Yield, (9.2) 0.12 g (56%); white solid; m.p. 90–91 °C. ¹H NMR (300 MHz, DMSO-*d*₆) δ 9.87 (s, 1H), 7.58 (d, *J* = 8.5 Hz, 1H), 6.72 (d, *J* = 8.5 Hz, 1H), 5.61 (s, 2H), 4.27 (q, *J* = 7.0 Hz, 1H), 4.16 (t, *J* = 4.3 Hz, 1H), 3.56 (s, 1H), 3.38 (s, *J* = 5.6 Hz, 1H), 2.98 (t, *J* = 6.1 Hz, 1H), 1.29 (t, *J* = 7.0 Hz, 1H); ¹³C NMR (75 MHz, DMSO-*d*₆) δ 162.05, 148.99, 138.61, 117.45, 109.24, 61.60, 42.57, 40.57, 27.82, 14.54. HRMS (ESI) *m/z* calcd for C₁₀H₁₅N₂O [M+H⁺] 179.1178 Da, found 179.1177 ± 0.0010 Da.

4.1.10 | Synthesis of 1-benzyl-5,6,7,8-tetrahydro-1,6-naphthyridin-2(1H)-one hydrochloride (9c)

It was prepared in full analogy to **9a/10a**, except that only *N*-alkylation product **9c** was obtained. Yield, 0.08 g (33%); white solid; m.p. 80–81 °C. ¹H NMR (300 MHz, DMSO-*d*₆) δ 9.76 (br.s, 2H), 7.40–7.29 (m, 3H), 7.26 (d, *J* = 7.0 Hz, 1H), 7.14 (d, *J* = 7.1 Hz, 2H), 6.49 (d, *J* = 9.3 Hz, 1H), 5.28 (s, 2H), 3.99 (br.s, 2H), 3.32–3.21 (m, 3H), 2.90 (br.s, 2H); ¹³C NMR (75 MHz, DMSO-*d*₆) δ 161.73, 140.58, 138.86, 136.64, 128.72, 127.23, 126.43, 117.98, 107.30, 45.41, 41.89, 39.36, 23.06. HRMS (ESI) *m/z* calcd for C₁₅H₁₇N₂O [M+H⁺] 241.1335 Da, found 241.1336 ± 0.0020 Da.

4.1.11 | Synthesis of 1-(3-fluorobenzyl)-5,6,7,8-tetrahydro-1,6-naphthyridin-2(1H)-one hydrochloride (9d)

It was prepared in full analogy with **9a/10a**, except that only *N*-alkylation product **9d** was obtained. Yield, 0.03 g (14%); white solid; m.p. 89–90 °C. ¹H NMR (300 MHz, DMSO-*d*₆) δ 9.86 (br.s, 2H), 7.38 (d, *J* = 9.4 Hz, 1H), 7.39–7.31 (m, 1H), 7.14–7.03 (m, 1H), 7.03–6.89 (m, 2H), 6.49 (d, *J* = 9.3 Hz, 1H), 5.28 (s, 2H), 3.99 (br.s, 2H), 3.33–3.22 (m, 2H), 2.91 (t, *J* = 5.1 Hz, 2H); ¹³C NMR (75 MHz, DMSO-*d*₆) δ 162.38 (d, *J* = 243.9 Hz), 161.75, 140.66, 139.65 (d, *J* = 7.4 Hz), 139.19, 130.81 (d, *J* = 8.4 Hz), 122.57 (d, *J* = 2.6 Hz), 117.94, 114.15 (d, *J* = 20.9 Hz), 113.36 (d, *J* = 22.1 Hz), 107.65, 45.20, 41.80, 39.32, 23.13. HRMS (ESI) *m/z* calcd for C₁₅H₁₆FN₂O [M+H⁺] 259.1241 Da, found 259.1240 ± 0.0020 Da.

4.1.12 | Synthesis of 1-(4-chlorobenzyl)-5,6,7,8-tetrahydro-1,6-naphthyridin-2(1H)-one hydrochloride (9e) and 2-[[4-chlorobenzyl]oxy]-5,6,7,8-tetrahydro-1,6-naphthyridine hydrochloride (10e)

They were prepared in full analogy with **9a/10a**.

9e: Yield, 0.026 g (9%); white solid; m.p. 107–108 °C. ¹H NMR (300 MHz, DMSO-*d*₆) δ 9.58 (br.s, 2H), 7.38 (dd, *J* = 10.7, 9.0 Hz, 3H), 7.18 (d, *J* = 8.4 Hz, 2H), 6.49 (d, *J* = 9.3 Hz, 1H), 5.27 (s, 2H), 3.99 (s, 2H), 3.27 (s, 2H), 2.89 (d, *J* = 5.5 Hz, 2H); ¹³C NMR (75 MHz, DMSO-

d_6) δ 161.7, 140.5, 138.9, 135.7, 131.8, 128.6, 128.5, 118.0, 107.4, 44.9, 41.9, 39.4, 23.1. HRMS (ESI) m/z calcd for $C_{15}H_{16}ClN_2O$ $[M+H^+]$ 275.7527 Da, found 275.7525 \pm 0.0010 Da.

10e: Yield, 0.12 g (41%); white solid; m.p. 105–106°C. 1H NMR (300 MHz, DMSO- d_6) δ 9.72 (br.s, 2H), 7.60 (d, J = 8.5 Hz, 1H), 7.45 (q, J = 8.6 Hz, 4H), 6.79 (d, J = 8.5 Hz, 1H), 5.31 (s, 2H), 4.18 (t, J = 4.2 Hz, 2H), 3.46–3.36 (m, 2H), 2.99 (t, J = 6.2 Hz, 2H); ^{13}C NMR (75 MHz, DMSO- d_6) δ 161.7, 149.1, 140.2, 138.6, 136.3, 130.0, 128.5, 117.9, 109.4, 42.7, 41.4, 39.4, 23.0. HRMS (ESI) m/z calcd for $C_{15}H_{16}ClN_2O$ $[M+H^+]$ 275.7527 Da, found 275.7526 \pm 0.0020 Da.

4.1.13 | Synthesis of 1-(4-fluorobenzyl)-5,6,7,8-tetrahydro-1,6-naphthyridin-2(1H)-one hydrochloride (9f) and 2-[(4-fluorobenzyl)oxy]-5,6,7,8-tetrahydro-1,6-naphthyridine hydrochloride (10f)

They were prepared in full analogy with **9a/10a**.

9f: Yield, 0.082 g (29%); white solid; m.p. 109–110°C. 1H NMR (300 MHz, DMSO- d_6) δ 9.54 (s, 2H), 7.35 (d, J = 9.4 Hz, 1H), 7.25–7.12 (m, 4H), 6.49 (d, J = 9.3 Hz, 1H), 5.26 (s, 2H), 3.99 (s, 2H), 3.28 (s, 2H), 2.90 (t, J = 5.7 Hz, 2H). HRMS (ESI) m/z calcd for $C_{15}H_{16}FN_2O$ $[M+H^+]$ 259.1241 Da, found 259.1239 \pm 0.0020 Da.

10f: Yield, 0.082 g (29%); white solid; m.p. 100–101°C. 1H NMR (300 MHz, DMSO- d_6) δ 9.83 (br.s, 2H), 7.59 (d, J = 8.5 Hz, 1H), 7.54–7.46 (m, 2H), 7.24–7.14 (m, 2H), 6.77 (d, J = 8.5 Hz, 1H), 5.30 (s, 2H), 4.17 (t, J = 4.2 Hz, 2H), 3.45–3.36 (m, 2H), 3.01 (t, J = 6.2 Hz, 2H); ^{13}C NMR (75 MHz, DMSO- d_6) δ 161.7, 161.3 (d, J = 242.9 Hz), 140.5, 138.9, 132.79 (d, J = 3.1 Hz), 128.6 (d, J = 8.2 Hz), 118.0, 115.4 (d, J = 21.5 Hz), 107.3, 44.8, 41.9, 39.4, 23.0. HRMS (ESI) m/z calcd for $C_{15}H_{16}FN_2O$ $[M+H^+]$ 259.1241 Da, found 259.1240 \pm 0.0015 Da.

4.1.14 | Synthesis of 1-(2-methoxyethyl)-5,6,7,8-tetrahydro-1,6-naphthyridin-2(1H)-one hydrochloride (9g) and 2-(2-methoxyethoxy)-5,6,7,8-tetrahydro-1,6-naphthyridine hydrochloride (10g)

They were prepared in full analogy with **9a/9b**, except for the use of 2-methoxyethyl bromide as an alkylating agent.

10g: Yield, 0.138 g (57%); white solid; m.p. 62–63°C. 1H NMR (300 MHz, DMSO- d_6) δ 9.91 (br.s, 2H), 7.58 (d, J = 8.5 Hz, 1H), 6.74 (d, J = 8.5 Hz, 1H), 4.34 (t, J = 4.6 Hz, 2H), 4.19–4.12 (m, 2H), 3.63 (t, J = 4.6 Hz, 2H), 3.43–3.33 (m, 2H), 3.28 (s, 3H), 2.99 (t, J = 6.1 Hz, 2H); ^{13}C NMR (75 MHz, DMSO- d_6) δ 161.9, 149.0, 138.6, 117.7, 109.3, 70.2, 64.8, 58.2, 42.4, 40.4, 27.8. HRMS (ESI) m/z calcd for $C_{11}H_{17}N_2O_2$ $[M+H^+]$ 209.1284 Da, found 209.1282 \pm 0.0020 Da.

9g: Yield, 0.05 g (21%); white solid; m.p. 66–67°C. 1H NMR (300 MHz, DMSO- d_6) δ 9.59 (s, 2H), 7.29 (d, J = 9.4 Hz, 1H), 6.39 (d, J = 9.3 Hz, 1H), 4.10 (t, J = 5.3 Hz, 2H), 3.99 (s, 2H), 3.54 (t, J = 5.3 Hz, 1H), 3.39–3.28 (m, 1H), 3.22 (s, 2H), 3.07 (t, J = 5.8 Hz, 1H); ^{13}C NMR (75 MHz, DMSO- d_6) δ 161.4, 140.9, 138.7, 117.8, 106.8, 69.6, 58.5,

43.1, 41.9, 30.8, 23.2. HRMS (ESI) m/z calcd for $C_{11}H_{17}N_2O_2$ $[M+H^+]$ 209.1284 Da, found 209.1284 \pm 0.0020 Da.

4.1.15 | Synthesis of 3-[4-[(3-[(2-fluorobenzyl)oxy]methyl]-1-methyl-1,4,6,7-tetrahydro-5H-pyrazolo-[4,3-c]pyridin-5-yl)methyl]benzyl]oxy]phenyl]-propanoic acid hydrochloride (16a) (LK01408)

8a (0.29 mmol, 0.077 g) was dissolved in dichloromethane (3 ml). Triethylamine (0.58 mmol, 0.08 ml) and *tert*-butyl 3-[4-[(4-formylbenzyl)oxy]phenyl]propanoate (**11**; 0.29 mmol, 0.1 g) were added. After 15 min of stirring, sodium triacetoxylborohydride (STAB; 1.17 mmol, 0.248 g) was added and the stirring continued for 36 h. The progress of the reaction was monitored using thin-layer chromatography and 10% methanol in chloroform as an eluent. The reaction mixture was washed with 5% aq. K_2CO_3 (5 ml) and water (2 \times 5 ml), dried over anhydrous Na_2SO_4 , filtered, and concentrated in vacuo. The crude reduction amination product was fractionated on silica gel using chloroform as an eluent. Fractions containing the target material were pooled and concentrated to dryness. The residue was dissolved in anhydrous 1,4-dioxane. A 4 M solution of HCl in 1,4-dioxane (2 ml) was added and the mixture was sonicated until a well-formed hydrochloride salt precipitate separated (18 h). The latter was filtered off, washed with ether, and air-dried to give the title compound. Yield, 0.09 g (53%); white solid; m.p. 123–124°C. 1H NMR (300 MHz, DMSO- d_6) δ 11.73 (br.s, 1H), 7.68 (d, J = 7.8 Hz, 2H), 7.48 (d, J = 7.8 Hz, 2H), 7.37–7.28 (m, 2H), 7.21–7.15 (m, 2H), 7.13 (d, J = 8.6 Hz, 2H), 6.91 (d, J = 8.3 Hz, 2H), 5.09 (s, 2H), 4.54–4.32 (m, 2H), 4.45 (s, 2H), 4.41 (s, 2H), 4.04 (br.s, 2H), 3.67 (s, 3H), 3.66–3.57 (m, 1H), 3.34 (br.s, 1H), 3.20–2.95 (m, 2H), 2.74 (t, J = 7.4 Hz, 2H), 2.48 (t, J = 7.4 Hz, 2H); ^{13}C NMR (75 MHz, DMSO- d_6) δ 173.6, 160.2 (d, J = 245.5 Hz), 156.6, 143.4, 138.6, 135.3, 133.2, 131.4, 130.3 (d, J = 4.4 Hz), 129.7 (d, J = 8.2 Hz), 129.2, 129.2, 127.7, 124.8 (d, J = 14.8 Hz), 124.3 (d, J = 3.5 Hz), 115.1 (d, J = 21.3 Hz), 114.6, 107.01, 68.8, 65.2 (d, J = 3.5 Hz), 64.9, 57.0, 48.2, 46.1, 35.6, 35.5, 29.5, 18.2. HRMS (ESI) m/z calcd for $C_{32}H_{35}FN_3O_4$ $[M+H^+]$ 544.2606 Da, found 544.2602 \pm 0.0010 Da.

4.1.16 | Synthesis of 3-[4-[(3-[(3-fluorobenzyl)oxy]methyl]-1-methyl-1,4,6,7-tetrahydro-5H-pyrazolo-[4,3-c]pyridin-5-yl)methyl]benzyl]oxy]phenyl]-propanoic acid hydrochloride (16b)

It was synthesized analogously to **16a** using **8b** (0.29 mmol, 0.081 g), triethylamine (0.58 mmol, 0.08 ml), *tert*-butyl 3-[4-[(4-formylbenzyl)oxy]phenyl]propanoate (**11**, 0.29 mmol, 0.1 g), and STAB (1.17 mmol, 0.248 g). Yield, 0.04 g (24%); white solid; m.p. 124–125°C. 1H NMR (300 MHz, DMSO- d_6) δ 11.41 (br.s, 1H), 7.65 (d, J = 7.8 Hz, 2H), 7.49 (d, J = 8.0 Hz, 2H), 7.43–7.34 (m, 1H), 7.13 (d, J = 8.6 Hz, 2H),

7.12–7.05 (m, 3H), 6.91 (d, $J = 8.6$ Hz, 2H), 5.09 (s, 2H), 4.53–4.34 (m, 2H), 4.42 (br.s, 4H), 4.11–3.99 (m, 2H), 3.69 (s, 3H), 3.67–3.61 (m, 1H), 3.40–3.26 (m, 1H), 3.12–2.97 (m, 2H), 2.74 (t, $J = 7.6$ Hz, 2H), 2.47 (t, $J = 7.6$ Hz, 2H); ^{13}C NMR (75 MHz, DMSO- d_6) δ 173.6, 162.1 (d, $J = 243.6$ Hz), 156.5, 143.4, 141.0 (d, $J = 7.3$ Hz), 138.7, 135.2, 133.2, 131.3, 130.2 (d, $J = 8.3$ Hz), 129.2, 129.1, 127.7, 123.3 (d, $J = 2.7$ Hz), 114.6, 114.1 (d, $J = 21.0$ Hz), 113.9 (d, $J = 21.5$ Hz), 107.0, 70.5 (d, $J = 1.8$ Hz), 68.7, 64.8, 57.1, 48.2, 46.5, 35.6, 35.5, 29.4, 18.2. HRMS (ESI) m/z calcd for $\text{C}_{32}\text{H}_{35}\text{FN}_3\text{O}_4$ [$\text{M}+\text{H}^+$] 544.2606 Da, found 544.2637 \pm 0.0010 Da.

4.1.17 | Synthesis 3-(4-((4-((3-((4-fluorophenoxy)methyl)-1-methyl-1,4,6,7-tetrahydro-5H-pyrazolo[4,3-c]pyridin-5-yl)methyl)benzyl)oxy)phenyl)propanoic acid hydrochloride (16c)

It was synthesized analogously to **16a** using **8d** (0.29 mmol, 0.081 g), triethylamine (0.58 mmol, 0.08 ml), *tert*-butyl 3-{4-[(4-formylbenzyl)oxy]phenyl}propanoate (**11**, 0.29 mmol, 0.1 g), and STAB (1.17 mmol, 0.248 g). Yield, 0.084 g (51%); white solid; m.p. 110–111°C. ^1H NMR (300 MHz, DMSO- d_6) δ 11.84 (br.s, 1H), 7.72 (d, $J = 7.9$ Hz, 2H), 7.51 (d, $J = 7.9$ Hz, 2H), 7.15–7.04 (m, 4H), 6.95–6.85 (m, 4H), 5.09 (s, 2H), 4.94 (s, 2H), 4.54–4.34 (m, 2H), 4.08 (br.s, 2H), 3.69 (s, 3H), 3.67–3.58 (m, 1H), 3.41–3.26 (m, 1H), 3.24–2.98 (m, 2H), 2.74 (t, $J = 7.5$ Hz, 2H), 2.47 (t, $J = 7.5$ Hz, 2H); ^{13}C NMR (75 MHz, DMSO- d_6) δ 173.8, 156.7 (d, $J = 236.3$ Hz), 156.6, 154.4 (d, $J = 1.8$ Hz), 142.4, 138.7, 135.6, 133.2, 131.5, 129.5, 129.3, 127.9, 116.0 (d, $J = 1.4$ Hz), 115.8 (d, $J = 16.6$ Hz), 114.6, 107.3, 68.8, 63.8, 56.9, 48.1, 46.1, 35.8, 35.6, 29.5, 18.2. HRMS (ESI) m/z calcd for $\text{C}_{31}\text{H}_{33}\text{FN}_3\text{O}_4$ [$\text{M}+\text{H}^+$] 530.2450 Da, found 530.2446 \pm 0.0020 Da.

4.1.18 | Synthesis of 3-[4-((4-((1-methyl-3-((4-methylpyridin-2-yl)oxy)methyl)-1,4,6,7-tetrahydro-5H-pyrazolo[4,3-c]pyridin-5-yl)methyl)benzyl)oxy)phenyl]propanoic acid hydrochloride (16d)

It was synthesized analogously to **16a** using **8c** (0.29 mmol, 0.07 g), triethylamine (0.58 mmol, 0.08 ml), *tert*-butyl 3-{4-[(4-formylbenzyl)oxy]phenyl}propanoate (**11**, 0.29 mmol, 0.1 g), and STAB (1.17 mmol, 0.248 g). Yield, 0.06 g (34%); white solid; m.p. 63–64°C. ^1H NMR (300 MHz, DMSO- d_6) δ 11.74 (br.s, 1H), 7.71 (d, $J = 7.8$ Hz, 2H), 7.52 (d, $J = 7.8$ Hz, 2H), 7.37 (d, $J = 6.6$ Hz, 1H), 7.14 (d, $J = 8.3$ Hz, 2H), 6.92 (d, $J = 8.4$ Hz, 2H), 6.28 (s, 1H), 6.18 (d, $J = 6.6$ Hz, 1H), 5.11 (s, 2H), 4.66 (d, $J = 6.3$ Hz, 2H), 4.49–4.36 (m, 2H), 4.21–4.05 (m, 2H), 3.70 (s, 3H), 3.68–3.61 (m, 1H), 3.39–3.22 (m, 1H), 3.14–3.02 (m, 2H), 2.75 (t, $J = 7.4$ Hz, 2H), 2.49–2.44 (m, 2H), 2.15 (s, 3H); ^{13}C NMR (75 MHz, DMSO- d_6) δ 173.5, 156.5, 154.3, 147.0, 138.6, 134.9, 134.8, 133.1, 131.3, 129.3, 129.1, 127.7, 116.7, 114.6, 110.3, 106.4, 79.1, 68.7, 57.0, 48.1, 46.7, 35.4, 35.3, 29.4, 21.0, 18.1. HRMS (ESI) m/z calcd for $\text{C}_{31}\text{H}_{35}\text{N}_4\text{O}_4$ [$\text{M}+\text{H}^+$] 527.2652 Da, found 527.2659 \pm 0.0020 Da.

4.1.19 | Synthesis of 3-[4-((4-((1-methyl-3-((4-(trifluoromethyl)benzyl)oxy)methyl)-1,4,6,7-tetrahydro-5H-pyrazolo[4,3-c]pyridin-5-yl)methyl)benzyl)oxy]phenyl]propanoic acid hydrochloride (16e)

It was synthesized analogously to **16a** using **9a** (0.14 mmol, 0.048 g), triethylamine (0.29 mmol, 0.04 ml), *tert*-butyl 3-{4-[(4-formylbenzyl)oxy]phenyl}propanoate (**11**, 0.145 mmol, 0.05 g), and STAB (0.585 mmol, 0.124 g). Yield, 0.03 g (33%); white solid; m.p. 123–124°C. ^1H NMR (300 MHz, DMSO- d_6) δ 11.31 (s, 1H), 7.69 (d, $J = 8.2$ Hz, 2H), 7.62 (d, $J = 8.0$ Hz, 2H), 7.52 (d, $J = 8.0$ Hz, 2H), 7.42–7.34 (m, 3H), 7.14 (d, $J = 8.5$ Hz, 2H), 6.92 (d, $J = 8.6$ Hz, 2H), 6.48 (d, $J = 9.4$ Hz, 1H), 5.35 (dd, $J = 59.2, 15.6$ Hz, 2H), 5.10 (s, 2H), 4.40 (br.s, 2H), 4.05 (br.s, 2H), 3.75–3.58 (m, 1H), 3.23–3.11 (m, 1H), 3.01 (br.s, 2H), 2.75 (t, $J = 7.5$ Hz, 2H), 2.48 (t, $J = 7.5$ Hz, 2H); ^{13}C NMR (75 MHz, DMSO- d_6) δ 173.7, 161.6, 156.6, 141.4, 140.4, 138.9, 138.8, 132.5, 131.4, 129.2, 127.9, 127.8 (d, $J = 31.6$ Hz), 127.2, 125.5 (d, $J = 2.9$ Hz), 124.2 (d, $J = 271.8$ Hz), 118.0, 114.6, 106.7, 68.7, 57.5, 49.4, 46.8, 45.4, 35.5, 29.5, 23.6. HRMS (ESI) m/z calcd for $\text{C}_{33}\text{H}_{32}\text{F}_3\text{N}_2\text{O}_4$ [$\text{M}+\text{H}^+$] 577.2309 Da, found 577.2309 \pm 0.0015 Da.

4.1.20 | Synthesis of 3-[4-((4-((1-ethyl-2-oxo-1,5,7,8-tetrahydro-1,6-naphthyridin-6(2H)-yl)methyl)benzyl)oxy)phenyl]propanoic acid hydrochloride (16f)

It was synthesized analogously to **16a** using **9b** (0.14 mmol, 0.03 g), triethylamine (0.29 mmol, 0.04 ml), *tert*-butyl 3-{4-[(4-formylbenzyl)oxy]phenyl}propanoate (**11**, 0.145 mmol, 0.5 g), and STAB (0.585 mmol, 0.124 g).

Yield, 0.03 g (42%); white solid; m.p. 122–123°C. ^1H NMR (300 MHz, DMSO- d_6) δ 11.33 (br.s, 1H), 7.66 (d, $J = 7.9$ Hz, 2H), 7.54 (d, $J = 8.0$ Hz, 2H), 7.25 (d, $J = 9.4$ Hz, 1H), 7.14 (d, $J = 8.5$ Hz, 2H), 6.93 (d, $J = 8.5$ Hz, 2H), 6.34 (d, $J = 9.3$ Hz, 1H), 5.13 (s, 2H), 4.50–4.38 (m, 2H), 4.03 (br.s, 2H), 3.96 (q, $J = 7.0$ Hz, 2H), 3.71–3.62 (m, 1H), 3.37–3.24 (m, 1H), 3.22–3.09 (m, 2H), 2.77 (t, $J = 7.5$ Hz, 2H), 2.48 (t, $J = 7.5$ Hz, 2H), 1.15 (t, $J = 6.9$ Hz, 3H); ^{13}C NMR (75 MHz, DMSO- d_6) δ 173.8, 161.1, 156.6, 140.0, 138.8, 138.2, 133.2, 131.5, 129.3, 129.1, 128.0, 117.8, 114.6, 106.0, 79.2, 68.7, 57.3, 49.4, 47.2, 35.6, 29.5, 23.1, 13.3. HRMS (ESI) m/z calcd for $\text{C}_{27}\text{H}_{31}\text{N}_2\text{O}_4$ [$\text{M}+\text{H}^+$] 447.2278 Da, found 447.2274 \pm 0.0010 Da.

4.1.21 | Synthesis of 3-[4-((4-((1-benzyl-2-oxo-1,5,7,8-tetrahydro-1,6-naphthyridin-6(2H)-yl)methyl)benzyl)oxy)phenyl]propanoic acid hydrochloride (16g)

It was synthesized analogously to **16a** using **9c** (0.29 mmol, 0.08 g), triethylamine (0.29 mmol, 0.08 ml), *tert*-butyl 3-{4-[(4-formylbenzyl)oxy]phenyl}propanoate (**11**, **10**; 0.29 mmol, 0.1 g), and STAB (1.17 mmol, 0.248 g). Yield, 0.03 g (20%); white solid; m.p. 106–107°C. ^1H NMR

(300 MHz, DMSO- d_6) δ 11.98 (br.s, 1H), 7.68 (d, J = 7.7 Hz, 2H), 7.49 (d, J = 7.7 Hz, 2H), 7.37–7.20 (m, 4H), 7.19–7.08 (m, 4H), 6.91 (d, J = 8.3 Hz, 2H), 6.45 (d, J = 9.3 Hz, 1H), 5.25 (br.s, 2H), 5.10 (s, 2H), 4.42 (br.s, 2H), 4.13–3.95 (m, 2H), 3.56 (br.s, 1H), 3.32–2.89 (m, 3H), 2.74 (t, J = 7.4 Hz, 2H), 2.48 (t, J = 7.4 Hz, 2H); ^{13}C NMR (75 MHz, DMSO- d_6) δ 173.7, 161.6, 156.6, 140.4, 138.7, 138.7, 136.5, 133.2, 131.5, 129.2, 129.0, 128.6, 127.8, 127.1, 126.4, 117.9, 114.6, 106.6, 68.7, 57.2, 49.1, 46.6, 45.7, 35.6, 29.5, 23.5. HRMS (ESI) m/z calcd for $\text{C}_{32}\text{H}_{33}\text{N}_2\text{O}_4$ [$\text{M}+\text{H}^+$] 509.2435 Da, found 509.2447 \pm 0.0020 Da.

4.1.22 | Synthesis 3-{4-[(4-{1-(3-fluorobenzyl)-2-oxo-1,5,7,8-tetrahydro-1,6-naphthyridin-6(2H)-yl]-methyl}benzyl)oxy]phenyl}propanoic acid hydrochloride (16h)

It was synthesized analogously to **16a** using **9d** (0.58 mmol, 0.15 g), triethylamine (1.09 mmol, 0.16 ml), *tert*-butyl 3-{4-[(4-formylbenzyl)oxy]phenyl}propanoate (**11**, 0.58 mmol, 0.2 g), and STAB (2.34 mmol, 0.496 g). Yield, 0.098 g (32%); white solid, m.p. 146–147°C. ^1H NMR (300 MHz, DMSO- d_6) δ 11.37 (br.s, 1H), 7.63 (d, J = 7.8 Hz, 2H), 7.52 (d, J = 7.8 Hz, 2H), 7.43–7.32 (m, 2H), 7.19–7.05 (m, 3H), 7.03–6.84 (m, 4H), 6.47 (d, J = 9.3 Hz, 1H), 5.43–5.14 (m, 2H), 5.10 (s, 2H), 4.41 (br.s, 2H), 4.04 (br.s, 2H), 3.67–3.53 (m, 1H), 3.31–3.17 (m, 1H), 3.03 (br.s, 2H), 2.74 (t, J = 7.3 Hz, 2H), 2.47 (t, J = 7.3 Hz, 2H); ^{13}C NMR (75 MHz, DMSO- d_6) δ 173.6, 162.2 (d, J = 243.8 Hz), 161.5, 156.5, 140.3, 139.4 (d, J = 7.2 Hz), 138.7, 138.6, 133.1, 131.34, 130.6 (d, J = 8.2 Hz), 129.1, 128.9, 127.8, 122.4 (d, J = 1.8 Hz), 117.9, 114.5, 113.9 (d, J = 20.8 Hz), 113.3 (d, J = 22.1 Hz), 106.6, 68.6, 64.8, 57.3, 49.1, 46.6, 35.5, 29.49, 23.4. HRMS (ESI) m/z calcd for $\text{C}_{32}\text{H}_{32}\text{FN}_2\text{O}_4$ [$\text{M}+\text{H}^+$] 527.2341 Da, found 527.2352 \pm 0.0015 Da.

4.1.23 | Synthesis of 3-{4-[(4-{2-[(4-(trifluoromethyl)benzyl)oxy]-7,8-dihydro-1,6-naphthyridin-6(5H)-yl]methyl}benzyl)oxy]phenyl}propanoic acid hydrochloride (16i)

It was synthesized analogously to **16a** using **10a** (0.29 mmol, 0.101 g), triethylamine (0.58 mmol, 0.08 ml), *tert*-butyl 3-{4-[(4-formylbenzyl)oxy]phenyl}propanoate (**11**, 0.29 mmol, 0.1 g), and STAB (1.17 mmol, 0.248 g). Yield, 0.1 g (56%); white solid; m.p. 128–129°C. ^1H NMR (300 MHz, DMSO- d_6) δ 11.56 (br.s, 1H), 7.77–7.64 (m, 6H), 7.61 (d, J = 8.6 Hz, 1H), 7.54 (d, J = 8.0 Hz, 2H), 7.14 (d, J = 8.4 Hz, 2H), 6.93 (d, J = 8.5 Hz, 2H), 6.82 (d, J = 8.5 Hz, 1H), 5.43 (s, 2H), 5.12 (s, 2H), 4.51–4.42 (m, 2H), 4.23 (br.s, 2H), 3.73–3.62 (m, 1H), 3.46–3.31 (m, 1H), 3.30–3.20 (m, 1H), 3.04–2.90 (m, 1H), 2.75 (t, J = 7.4 Hz, 2H), 2.49 (t, J = 7.4 Hz, 2H); ^{13}C NMR (75 MHz, DMSO- d_6) δ 173.9, 161.8, 156.6, 148.9, 138.8, 138.6, 133.2, 131.6, 129.3, 129.2, 128.4, 128.3 (q, J = 31.8 Hz), 127.5, 125.3 (q, J = 3.7 Hz), 124.3 (q, J = 272.1 Hz), 117.3, 114.6, 109.4, 68.7, 66.1, 57.9, 50.3, 48.3, 35.6, 29.5, 28.1. HRMS (ESI) m/z calcd for $\text{C}_{33}\text{H}_{32}\text{F}_3\text{N}_2\text{O}_4$ [$\text{M}+\text{H}^+$] 577.2309 Da, found 577.2331 \pm 0.0020 Da.

4.1.24 | Synthesis of 3-{4-[(4-{2-[(4-chlorobenzyl)-oxy]-7,8-dihydro-1,6-naphthyridin-6(5H)-yl]methyl}benzyl)oxy]phenyl}propanoic acid hydrochloride (16j)

It was synthesized analogously to **16a** using **10e** (0.58 mmol, 0.091 g), triethylamine (1.09 mmol, 0.16 ml), *tert*-butyl 3-{4-[(4-formylbenzyl)oxy]phenyl}propanoate (**11**, 0.58 mmol, 0.2 g), and STAB (2.34 mmol, 0.496 g). Yield, 0.05 g (16%); white solid; m.p. 166–167°C. ^1H NMR (300 MHz, DMSO- d_6) δ 11.33 (br.s, 1H), 7.68 (d, J = 8.0 Hz, 2H), 7.59 (d, J = 8.6 Hz, 1H), 7.54 (d, J = 8.0 Hz, 2H), 7.45 (q, J = 8.6 Hz, 4H), 7.15 (d, J = 8.5 Hz, 2H), 6.93 (d, J = 8.5 Hz, 2H), 6.78 (d, J = 8.5 Hz, 1H), 5.32 (s, 2H), 5.11 (s, 2H), 4.53–4.40 (m, 2H), 4.24 (br.s, 2H), 3.49–3.33 (m, 2H), 3.31–3.17 (m, 1H), 3.07–2.90 (m, 1H), 2.75 (t, J = 7.5 Hz, 2H), 2.48 (t, J = 7.5 Hz, 2H); ^{13}C NMR (75 MHz, DMSO- d_6) δ 174.0, 161.9, 156.6, 148.8, 138.8, 138.5, 136.2, 133.2, 132.4, 131.5, 130.0, 129.3, 129.2, 128.4, 128.0, 117.2, 114.7, 109.4, 68.7, 66.2, 58.0, 50.4, 48.4, 35.6, 29.5, 28.1. HRMS (ESI) m/z calcd for $\text{C}_{32}\text{H}_{32}\text{ClN}_2\text{O}_4$ [$\text{M}+\text{H}^+$] 543.2045 Da, found 543.2063 \pm 0.0015 Da.

4.1.25 | Synthesis of 3-{4-[(4-{2-[(4-fluorobenzyl)-oxy]-7,8-dihydro-1,6-naphthyridin-6(5H)-yl]methyl}benzyl)oxy]phenyl}propanoic acid hydrochloride (16k)

It was synthesized analogously to **16a** using **10f** (0.58 mmol, 0.091 g), triethylamine (1.09 mmol, 0.16 ml), *tert*-butyl 3-{4-[(4-formylbenzyl)oxy]phenyl}propanoate (**11**, 0.58 mmol, 0.2 g), and STAB (2.34 mmol, 0.496 g). Yield, 0.09 g (27%); white solid; m.p. 220–221°C. ^1H NMR (300 MHz, DMSO- d_6) δ 10.74 (br.s, 1H), 7.66–7.60 (m, 2H), 7.59–7.46 (m, 5H), 7.21 (d, J = 8.9 Hz, 2H), 7.18–7.09 (m, 2H), 6.92 (d, J = 8.7 Hz, 2H), 6.78 (d, J = 8.5 Hz, 1H), 5.30 (s, 2H), 5.12 (s, 2H), 4.48 (br.s, 2H), 4.26 (br.s, 2H), 3.76–3.59 (m, 1H), 3.25–3.12 (m, 1H), 3.08–2.95 (m, 2H), 2.75 (t, J = 7.5 Hz, 2H), 2.48 (t, J = 7.5 Hz, 2H); ^{13}C NMR (75 MHz, DMSO- d_6) δ 173.8, 162.0, 161.7 (d, J = 243.5 Hz), 156.6, 148.7, 138.8, 138.4, 133.3 (d, J = 7.2 Hz), 131.4, 130.3 (d, J = 8.3 Hz), 129.3, 129.2, 129.1, 127.9, 117.0, 115.1 (d, J = 21.3 Hz), 114.6, 109.4, 68.7, 66.3, 57.9, 50.4, 48.4, 35.5, 29.5, 28.0. HRMS (ESI) m/z calcd for $\text{C}_{32}\text{H}_{32}\text{FN}_2\text{O}_4$ [$\text{M}+\text{H}^+$] 527.2341 Da, found 527.2363 \pm 0.0020 Da.

4.1.26 | Synthesis of 3-{4-[(4-{2-(2-methoxyethoxy)-7,8-dihydro-1,6-naphthyridin-6(5H)-yl]methyl}benzyl)oxy]phenyl}propanoic acid hydrochloride (16l)

It was synthesized analogously to **16a** using **10g** (0.29 mmol, 0.071 g), triethylamine (0.58 mmol, 0.08 ml), *tert*-butyl 3-{4-[(4-formylbenzyl)oxy]phenyl}propanoate (**11**, 0.29 mmol, 0.1 g), and STAB (1.17 mmol, 0.248 g). Yield, 0.02 g (14%); white solid; m.p. 89–90°C. ^1H NMR (300 MHz, DMSO) δ 11.60 (br.s, 1H), 7.70 (d, J = 7.5 Hz, 2H), 7.60–7.48 (m, 3H), 7.14 (d, J = 7.9 Hz, 2H), 6.93 (d, J = 8.1 Hz, 2H), 6.71 (d, J = 8.3 Hz, 1H), 5.11 (s, 2H), 4.45 (br.s, 2H), 4.35 (br.s, 2H), 4.22 (br.s,

2H), 3.64 (s, 3H), 3.42–3.31 (m, 2H), 3.28 (s, 3H), 3.04–2.91 (m, 1H), 2.75 (t, $J = 6.9$ Hz, 2H), 2.48 (t, $J = 6.9$ Hz, 2H); ^{13}C NMR (75 MHz, DMSO) δ 174.0, 162.3, 156.7, 148.8, 138.8, 138.4, 133.3, 131.6, 129.4, 129.3, 128.1, 116.8, 114.7, 109.4, 70.2, 68.8, 64.8, 58.2, 57.9, 50.4, 48.4, 35.7, 29.6, 28.1. HRMS (ESI) m/z calcd for $\text{C}_{28}\text{H}_{33}\text{N}_2\text{O}_5$ $[\text{M}+\text{H}^+]$ 477.2384 Da, found 477.2401 \pm 0.0010 Da.

4.2 | Biological assays

4.2.1 | In vitro FFA1 activation assay

CHO cells stably expressing human FFA1 (stable CHO-GPR40 line created at Enamine Ltd.) were seeded (12,500 cells/well) into 384-well black-wall, clear-bottom microtiter plates 24 h before assay. Cells were loaded for 1 h with fluorescent calcium dye (Fluo-8 Calcium Assay Kit, ab112129; Abcam) and tested using a fluorometric imaging plate reader (FLIPR Tetra® High-Throughput Cellular Screening System; Molecular Devices Corp.). The maximum change in fluorescence over the baseline was used to determine the agonist response. A potent and selective agonist for FFA1 GW9508 (S8014; Selleckchem) was tested with the test compounds as a positive control. The concentration–response curve data were fitted using Molecular Devices ScreenWorks® System Control Software (Molecular Devices).

4.2.2 | Caco-2 permeability assay

Caco-2 cells (human colorectal adenocarcinoma line, Cat. HTB-37; ATCC) were cultivated in a Dulbecco's modified Eagle's medium supplemented with 10% fetal bovine serum (FBS), 1% nonessential amino acids solution, and 0.1% penicillin/streptomycin in a humidified atmosphere at 37°C in 5% CO_2 to 70–80% confluence, which were then seeded at 1×10^5 cells/well on 24-well semipermeable insert plates (Millicell Multiwell PCF 0.4 μm or similar). The medium was changed every 2 days. After 10 days of cell growth, the integrity of differentiated Caco-2 monolayers was verified by transepithelial electrical resistance (TEER) measurements using Millicell-ERS Voltohmmeter (Millipore EMD). Caco-2 cell monolayers were considered acceptable for transport studies if the final values of TEER were greater than 1000 $\text{ohm}\cdot\text{cm}^{-2}$. For the permeability studies, the 24-well insert plate was removed from its feeder plate and placed in a new sterile 24-well receiver plate. The cell layer was washed twice with phosphate-buffered saline. Aliquots (300 μl) of the test compound solution (in duplicates, at 10 μM , in Hanks' balanced salt solution with 5.6 mM glucose buffered with 10 mM HEPES, pH 7.4) were added into the apical compartments of the trans-well insert and 1000 μl of the same buffer was added to the basolateral compartments. The plates were then incubated for 2 h at 37°C. High, low, and intermediate permeability controls (atenolol, propranolol, quinidine) were run with every experimental batch to verify assay validity. The concentrations of the compounds tested in the A–B permeability assay were determined using the HPLC-MS method. The LC system comprised a Shimadzu liquid chromatograph equipped with isocratic pumps (Shimadzu LC-10ADvp),

an autosampler (Shimadzu SIL-HTc), a switching valve (FCV-14AH), and a degasser (Shimadzu DGU-14A). The mass spectrometric analysis was performed using API 3000 (triple-quadrupole) instrument from PE Sciex with electrospray interface. The data acquisition and system control were performed using Analyst 1.5.2 software from PE Sciex.

The formula for calculating P_{app} (expressed in $10^{-6} \text{ cm}\cdot\text{s}^{-1}$) is as follows:

$$P_{\text{app}} = (\text{VA}/((\text{Area}) \times (\text{Time}))) \times ([\text{drug}]_{\text{acc}}/[\text{drug}]_{\text{init,d}}),$$

where VA is the volume of transport buffer in the acceptor well; Area, the surface area of the insert (equal to effective growth area of the insert); Time, the time of the assay; $[\text{drug}]_{\text{acc}}$, the concentration of the test compound in the acceptor well; and $[\text{drug}]_{\text{init,d}}$, the initial concentration of the test compound in the donor well.

4.2.3 | Insulin secretion assay in INS1E cells

Cell culture

Rat insulinoma (clonal INS-1E cells isolated from the parental INS-1 line, Cat. C0018009; AddexBio) was cultured in RPMI-1640 medium containing 11 mM glucose, supplemented with 10% fetal bovine serum, 100 units/ml penicillin, 100 $\mu\text{g}/\text{ml}$ streptomycin, 10 mM HEPES, 1 mM sodium pyruvate, and 50 μM β -mercaptoethanol. Cells were maintained in the logarithmic growth phase at 37°C in a humidified atmosphere containing 5% CO_2 .

Insulin secretion assay

INS1E cells were seeded in 96-well plates at the density of 5×10^4 cells/well and cultured at 37°C and 5% CO_2 for 72 h. The cell medium was replaced with glucose-free RPMI 1640 containing 1% FBS for 1 h. Next, cells were washed with Krebs–Ringer bicarbonate HEPES buffer (KRBH; 129 mmol/l NaCl, 4.8 mmol/l KCl, 2.5 mmol/l CaCl_2 , 1.2 mmol/l MgSO_4 , 1.2 mmol/l KH_2PO_4 , 5 mmol/l NaHCO_3 , and 10 mmol/l HEPES, pH 7.4) containing 0.1% BSA (fatty acid-free) with 0.5 mM glucose and then stimulated with a test or reference compounds in KRBH with 0.1% BSA for 2 h in the presence of 0.5 or 16.7 mM glucose. DMSO was used as a negative control and GW9508 (10 μM) as a positive control (final DMSO concentration, 0.5%). The test compounds were added at 10 μM concentration. Supernatants (100 μl) were harvested from all wells to determine insulin levels.

The secreted insulin in the cell culture medium of INS1E cells was measured using the HTRF Assay Kit (Cat. 62IN1PEG; Cisbio Bioassays) according to manufacturer's recommendations. Briefly, 5 μl of the test or control sample was added into the respective wells of a black 384-well microplate and supplemented with 25 μl of anti-insulin- Eu^{3+} Cryptate donor antibody and 50 μl of anti-insulin-XL665 antibody. The plate was incubated overnight at room temperature and the HTRF signal was read with the excitation at 317 nm wavelength and emissions at 620 nm (for donor) and 665 nm (for acceptor). The results were expressed as the ratio of 665 nm/620 nm. For insulin quantification, a calibration curve was constructed using the insulin standard included in the kit.

4.3 | Docking studies

Protein structure (FFA1) was downloaded from RCSB Protein Data Bank (PDB ID: 4PHU). The protein structure was corrected and pre-processed using Schrödinger Protein PrepWizard: missing atoms were added, alternate residue positions were defined, and the hydrogen bonding network was further optimized by reorientating hydroxyls, amides, and imidazole rings (including histidines).^[26] The docking protocol was evaluated using the reference structure from model 4PHU. Redocking results in comparison to the native binding mode displayed a root mean square deviation <math><1.8 \text{ \AA}</math>. For each of the best docking solutions, MM-GBSA free energy components were calculated. Protein surface characteristics (hydrophobic properties) were calculated using the Schrödinger Protein Surface Analyzer. Molecular docking was processed with the use of Schrödinger Glide software.^[27] All of the software tools mentioned above are part of the Schrödinger Suite 2019-4.

ACKNOWLEDGMENTS

This study was supported by the Russian Foundation for Basic Research (project grant 19-33-90169). Alexander Safrygin is thankful for the postdoctoral fellowship from Saint Petersburg State University. The authors are grateful to the Center for Chemical Analysis and Materials Research of Saint Petersburg State University for providing high-resolution mass spectrometry data.

CONFLICTS OF INTERESTS

The authors declare that there are no conflicts of interests.

ORCID

Sergey Zozulya  <http://orcid.org/0000-0002-1179-2993>

Maxim Gureev  <http://orcid.org/0000-0002-0385-922X>

Alexander Safrygin  <http://orcid.org/0000-0002-2436-9019>

Mikhail Krasavin  <http://orcid.org/0000-0002-0200-4772>

REFERENCES

- [1] C. P. Briscoe, M. Tadayyon, J. L. Andrews, W. G. Benson, J. K. Chambers, M. M. Eilert, C. Ellis, N. A. Elshourbagy, A. S. Goetz, D. T. Minnick, P. R. Murdock, H. R. Sauls, U. Shabon, L. D. Spinage, J. C. Strum, P. G. Szekeres, K. B. Tan, J. M. Way, D. M. Ignar, S. Wilson, A. I. Muir, *J. Biol. Chem.* **2003**, 278, 11303.
- [2] M. Kebede, M. Ferdaoussi, A. Mancini, T. Alquier, R. N. Kulkarni, M. D. Walker, V. Poitout, *Proc. Natl. Acad. Sci. U.S.A.* **2012**, 109, 2376.
- [3] K. R. Waterson, B. D. Hudson, T. Ulven, G. Milligan, *Front. Endocrinol.* **2014**, 5, 137.
- [4] E. Defossa, M. Wagner, *Bioorg. Med. Chem. Lett.* **2014**, 24, 2991.
- [5] (a) Z. Li, Z. Zhou, L. Zhang, *Exp. Opin. Ther. Pat.* **2020**, 30, 27; (b) G. Milligan, B. Shimpukade, T. Ulven, B. D. Hudson, *Chem. Rev.* **2017**, 117, 67; (c) Z. Li, X. Xu, W. Huang, H. Qian, *Med. Res. Rev.* **2018**, 38, 381; (d) Z. Li, Q. Qiu, X. Geng, J. Yang, W. Huang, H. Qian, *Expert Opin. Invest. Drugs* **2016**, 25, 871
- [6] K. Kaku, K. Enya, R. Nakaya, T. Ohira, R. Matsuno, *Diabetes, Obes. Metab.* **2015**, 17, 675.
- [7] T. Yamashima, *Prog. Lipid Res.* **2015**, 58, 40.
- [8] Z. Weng, K. Wang, H. Li, Q. Shi, *Oncotarget* **2015**, 6, 17013.
- [9] A. D. Mancini, V. Poitout, *Diabetes, Obes. Metab.* **2015**, 17, 622.
- [10] A. Ichimura, A. Hirasawa, T. Hara, G. Tsugimoto, *Prostaglandins Other Lipid Mediators* **2009**, 89, 82.

- [11] I. Zahanich, I. Kondratov, V. Naumchyk, Y. Kheylik, M. Platonov, S. Zozulya, M. Krasavin, *Bioorg. Med. Chem. Lett.* **2015**, 25, 3105.
- [12] J. Liu, Y. Wang, Z. Ma, M. Schmitt, L. Zhu, S. P. Brown, P. J. Dransfield, Y. Sun, R. Sharma, Q. Guo, R. Zhuang, J. Zhang, J. Luo, G. R. Tonn, S. Wong, G. Swaminath, J. C. Medina, D. C.-H. Lin, J. B. Houze, *ACS Med. Chem. Lett.* **2014**, 5, 517.
- [13] X. Du, P. J. Dransfield, D. C.-H. Lin, S. Wong, Y. Wang, Z. Wang, T. Kohn, M. Yu, S. P. Brown, M. Vimolratana, L. Zhu, A.-R. Li, Y. Su, X. Jiao, J. Liu, G. Swaminath, T. Tran, J. Luo, R. Zhuang, J. Zhang, Q. Guo, F. Li, R. Connors, J. C. Medina, J. B. Houze, *ACS Med. Chem. Lett.* **2014**, 5, 384.
- [14] (a) M. Krasavin, A. Lukin, N. Zhurilo, A. Kovalenko, I. Zahanich, S. Zozulya, *J. Enzyme Inhib. Med. Chem.* **2016**, 31, 1404; (b) M. Krasavin, A. Lukin, N. Zhurilo, A. Kovalenko, I. Zahanich, S. Zozulya, D. Moore, I. G. Tikhonova, *Bioorg. Med. Chem.* **2016**, 24, 2954; (c) M. Krasavin, A. Lukin, A. Bakholdina, N. Zhurilo, O. Onopchenko, P. Borysko, S. Zozulya, D. Moore, I. G. Tikhonova, *Eur. J. Med. Chem.* **2017**, 140, 229
- [15] M. Krasavin, A. Lukin, D. Bagnyukova, N. Zhurilo, I. Zahanich, S. Zozulya, J. Ihalainen, M. M. Forsberg, M. Lehtonen, J. Rautio, D. Moore, I. G. Tikhonova, *Bioorg. Med. Chem.* **2016**, 24, 5481.
- [16] M. Krasavin, A. Lukin, D. Bagnyukova, N. Zhurilo, I. Zahanich, S. Zozulya, *J. Enzyme Inhib. Med. Chem.* **2017**, 32, 29.
- [17] M. Krasavin, A. Lukin, D. Bagnyukova, N. Zhurilo, A. Golovanov, S. Zozulya, I. Zahanich, D. Moore, I. G. Tikhonova, *Eur. J. Med. Chem.* **2017**, 127, 357.
- [18] M. Krasavin, A. Lukin, N. Zhurilo, D. Bagnyukova, *Lett. Org. Chem.* **2016**, 13, 491.
- [19] M. P. Arrington, R. Liu, A. T. Hopper, R. D. Conticello, T. M. Nguyen, C. M. Gauss, R. Burli, S. A. Hitchcock, E. Hu, R. Kunz, T. Nixey, S. Rumpfelt, *PCT Int. Appl. WO 2007098169*; *Chem. Abstr.* **2007**, 147, 301187.
- [20] A. C.-M., Daugan, *PCT Int. Pat. Appl. WO 2009056556*; *Chem. Abstr.* **2009**, 150, 494845.
- [21] C. P. Briscoe, A. J. Peat, S. C. McKeown, D. F. Corbett, A. S. Goetz, T. R. Littleton, D. C. McCoy, T. P. Kenakin, J. L. Andrews, C. Ammalá, J. A. Fornwald, D. M. Ignar, S. Jenkinson, *Br. J. Pharmacol.* **2006**, 148, 619.
- [22] I. J. Hidalgo, T. J. Raub, R. T. Borchard, *Gastroenterology* **1989**, 96, 736.
- [23] Z. Wang, C. E. Hop, K. H. Leung, J. Pang, *J. Mass Spectrom.* **2000**, 35, 71.
- [24] T. Špaček, J. Šantorová, K. Zacharovová, Z. Berková, L. Hlavatá, F. Saudek, P. Ježeka, *Int. J. Biochem. Cell Biol.* **2008**, 40, 1522.
- [25] T. L. Levien, D. E. Baker, R. K. Campbell, J. R. White, *Ann. Pharmacother.* **2001**, 35, 1426.
- [26] G. M. Sastry, M. Adzhigirey, T. Day, R. Annabhimoju, W. Sherman, *J. Comput. Aided Mol. Des.* **2013**, 27, 221.
- [27] R. A. Friesner, J. L. Banks, R. B. Murphy, T. A. Halgren, J. J. Klicic, D. T. Mainz, M. P. Repasky, E. H. Knoll, M. Shelley, J. K. Perry, D. E. Shaw, P. Francis, P. S. Shenkin, *J. Med. Chem.* **2004**, 47, 1739.

SUPPORTING INFORMATION

Additional supporting information may be found online in the supporting information tab for this article.

How to cite this article: Lukin A, Bakholdina A, Zhurilo N, et al. Exploration of the nitrogen heterocyclic periphery around the core of the advanced FFA1 agonist fasiglifam (TAK-875). *Arch Pharm.* 2020;e2000275.
<https://doi.org/10.1002/ardp.202000275>